Renormalization Group Approaches
to
Strongly Correlated Electron and Electron-Phonon Systems

Outline

1. The Application of NRG-DMFT to the Hubbard-Holstein Models

2. Polaron Bands in a a Many-electron System

3. Calculation of Renormalised Parameters from NRG Calculations

4. De-renormalisation as a function of Magnetic Field Strength

5. Applications within a Renormalised Perturbation Expansion.

4. Spin and Charge Dynamics in an Impurity Model

5. Potential Application to Heavy Fermions and Quantum Critical Points.

Collaborators:

Winfried Koller
Dietrich Meyer,
Akira Oguri
Ralf Bulla
Johannes Bauer
Yoshiaki Ono.

Holstein-Hubbard Model

$$H = -\sum_{<i,j>,\sigma} t(c_{i\sigma}^{\dagger} c_{j\sigma} + h.c.) + U \sum_i c_{i\uparrow}^{\dagger} c_{i\uparrow} c_{i\downarrow}^{\dagger} c_{i\downarrow}$$

$$+g \sum_i \left(\sum_{\sigma} n_{i,\sigma} - 1 \right) (b_i^{\dagger} + b_i) + \sum_i \omega_0 b_i^{\dagger} b_i$$

Four significant parameters, band-width $2D = 4t$, local interaction U, electron-phonon interaction g, and phonon frequency ω_0.

Strong Correlation Physics that can be studied by this model:

- Metal-Insulator Transitions at half-filling
- Bipolaron Formation
- Polaronic Formation
- Charge Order
- Antiferromagnetism
- Superconductivity

DMFT-NRG for Lattice Models

Hubbard Model and Metal Insulator Transition

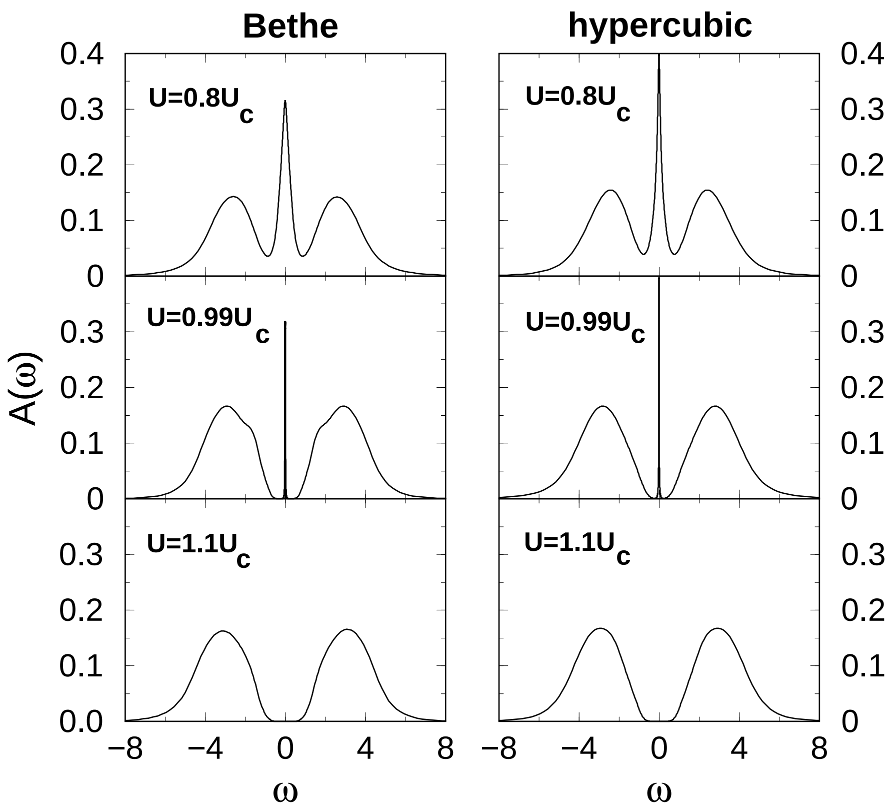

Results for Spectral Density of Half-filled Hubbard Model as a function of U of Ralf Bulla. Critical value $U_c/D = 2.93$ $(W = 2D)$.

Results for Half-filled Holstein Model

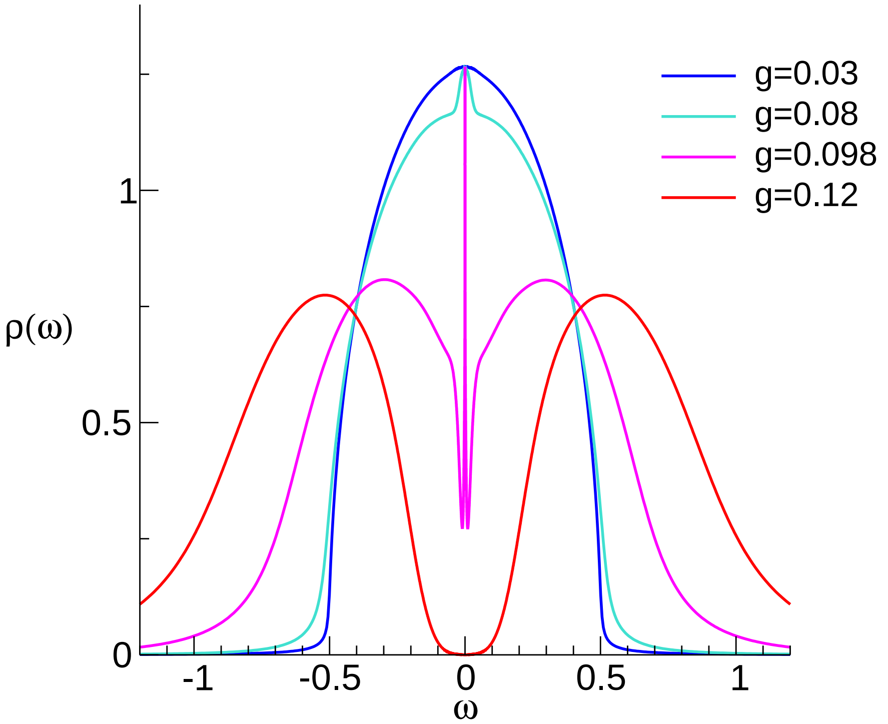

The effect of increasing g on the interacting density of states.

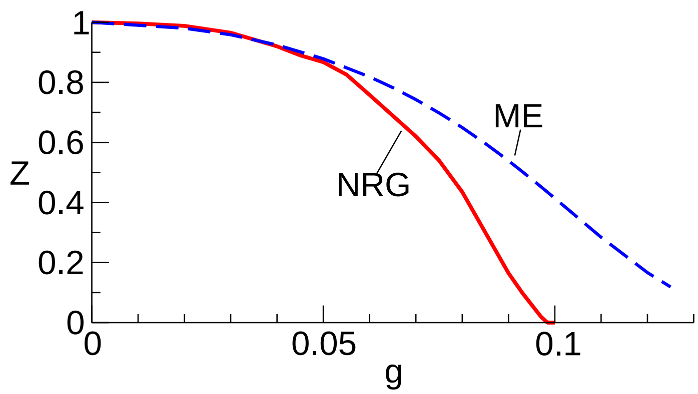

The decrease of quasiparticle weight factor z with increase of g.

Phonon Spectra for the Holstein Model at Half-filling

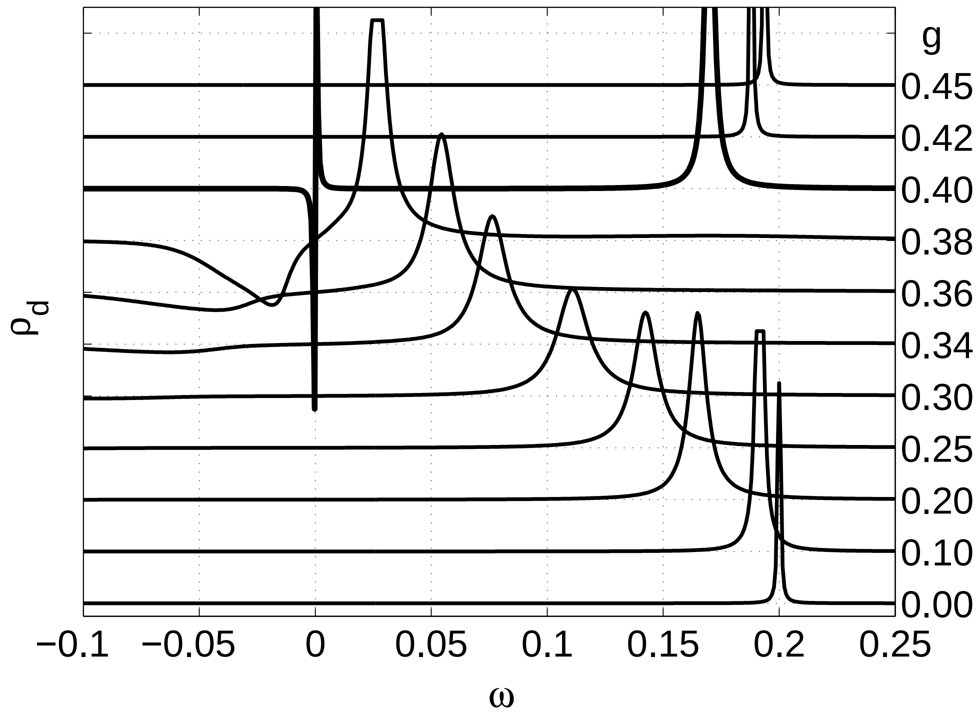

This shows the softening of the phonon spectrum with increase of g for the Holstein model (U=0) and the rehardening after the transition to a bipolaronic state. There is a regime near the transition where two peaks in the spectrum can be seen.

Quasiparticle Interactions for the Holstein Model

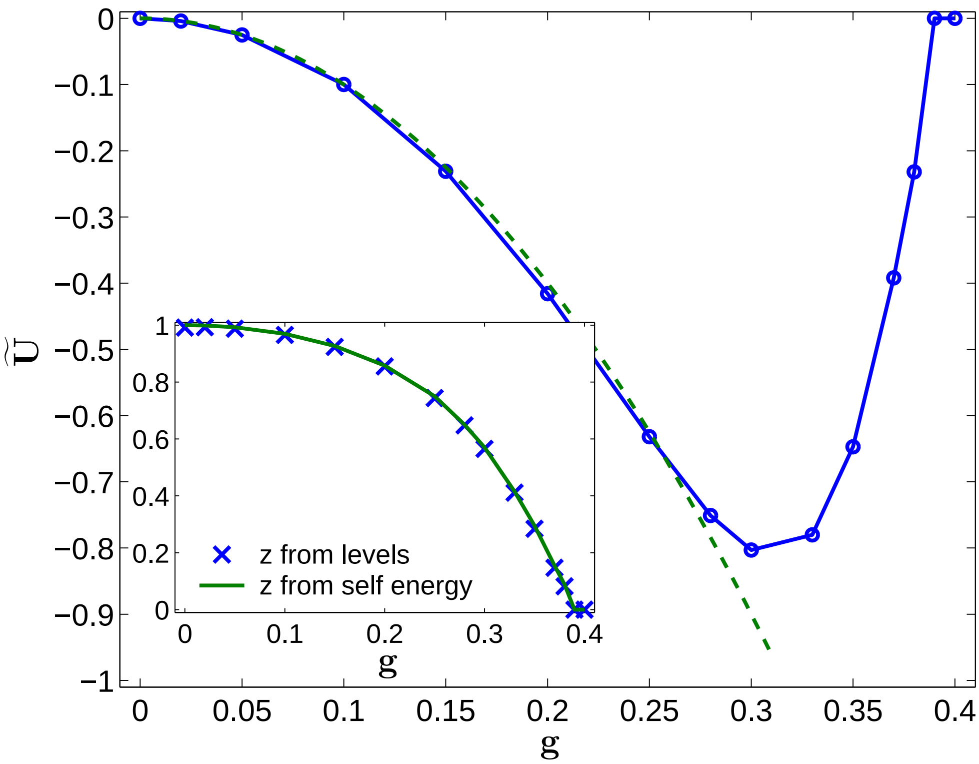

From an analysis of the fixed point we can deduce both z and the local quasiparticle interaction $\tilde{U}$. The value of z deduced in in complete agreement with that deduced by differentiating the self-energy $\Sigma(\omega)$. The value of $\tilde{U}$ is new information. Note that the value of $\tilde{U}$ behaves as expected becoming more negative initially and then less negative as the bipolarons form.

Effective interaction due to single phonon exchange:

$$U_{\rm eff} = U - \frac{2g^2}{\omega_0}$$

Phase Diagram for Hubbard-Holstein Model

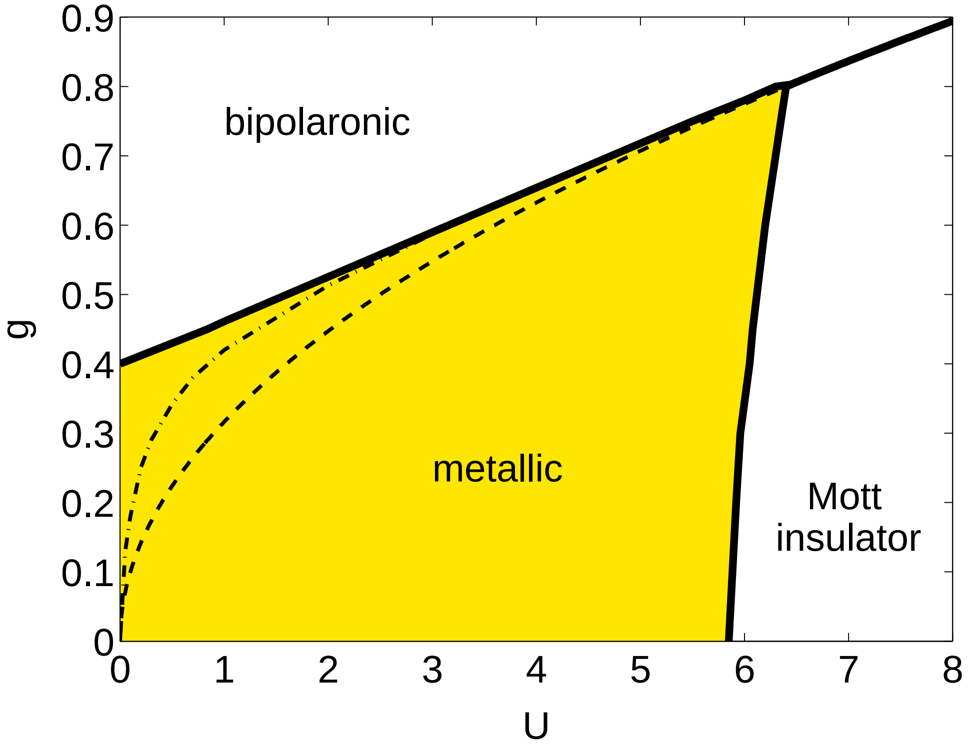

The possibility of a broken symmetry state (charge order or antiferromagnetism) is not included.

Density of States for H-H Model U=5

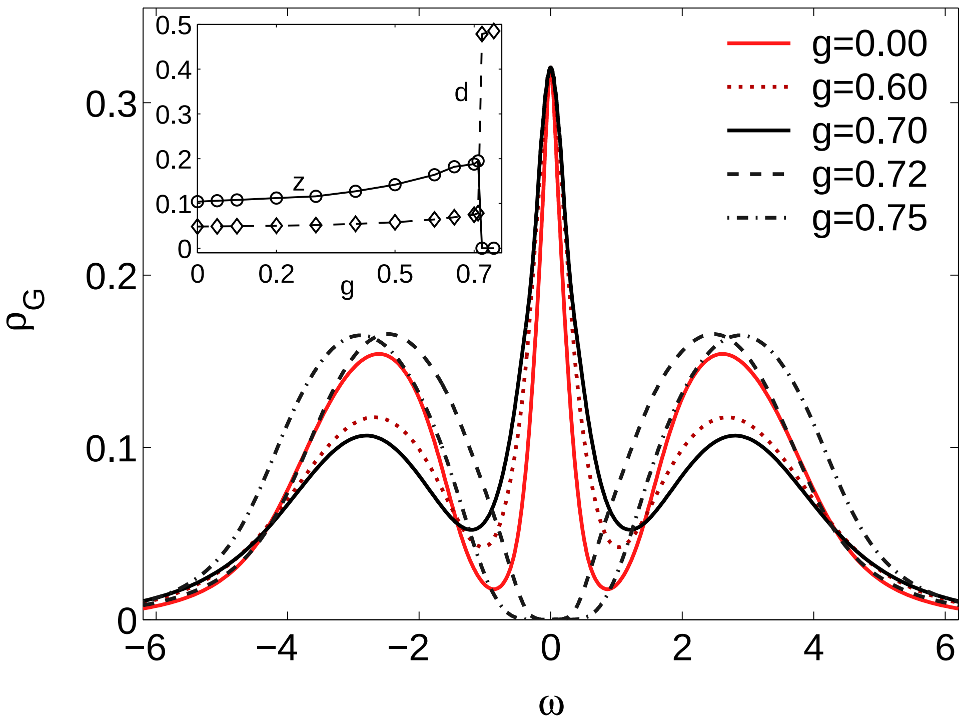

Here we start with strongly renormalized quasiparticles (small z and narrow quasiparticle peak at the Fermi level). As g increases z increases slowly but for large g there is a first order transition to a bipolaronic state.

The Hole Doped Holstein Model

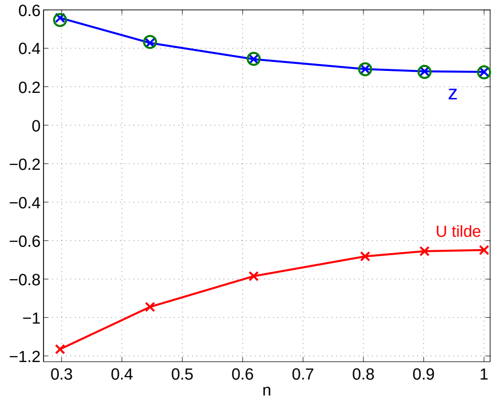

Quasiparticle weight z as a function of filling.

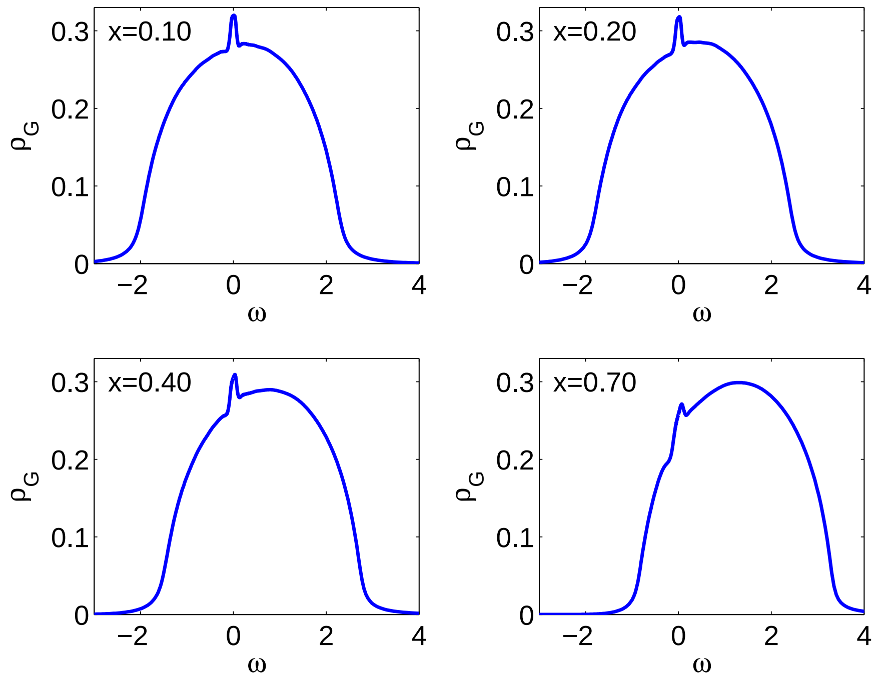

Fixed $g = 0.35$ and increased doping x. Quasiparticle peak tied to the Fermi level.

Polaronic Quasiparticles in the Holstein-Hubbard Model

Do pure polaronic excitations exist in the Holstein-Hubbard model? Polarons have been studied almost exclusively for one or two electrons in models without spin, such as the original Holstein model. In these models there is no effective local interaction inducing bipolaron formation, and no complications phase space restrictions due to the other electrons.

Conditions favouring polaronic excitations:

- Large U to inhibit local bipolaron formation

- Away from half-filling where spin fluctuations dominate.

We take $U = 6$ and look near quarter filling, and increase the electron-phonon coupling g

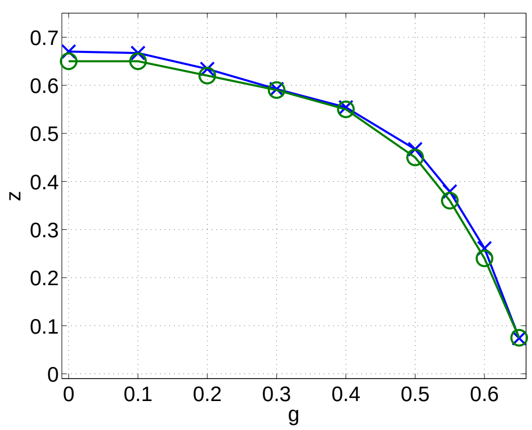

Quasiparticle weight z as a function of g from t self-energy ($\circ$) and from renormalised parameters ($\times$).
The quasiparticles are being renormalized due to polaronic effects!

Polaronic Quasiparticles

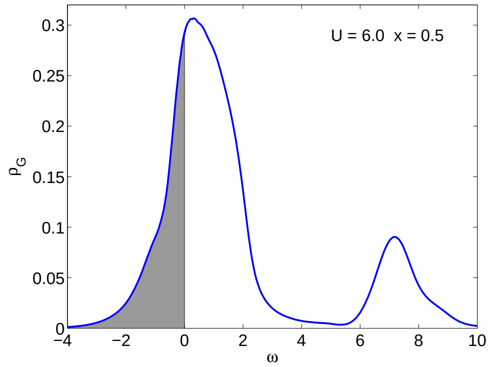

Quarter Filled Hubbard for $U = 6$ and $g = 0$.

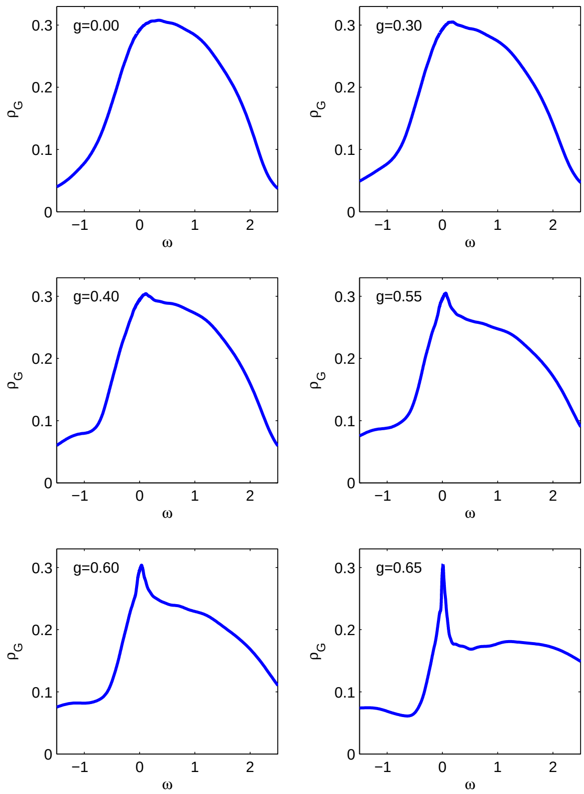

Narrow polaronic band develops at the Fermi level for $U = 6$ and increasing values of g.

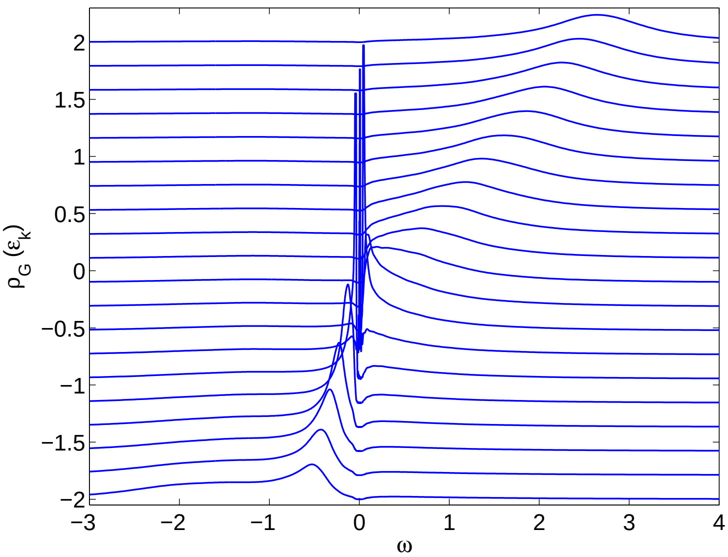

Plot of $\rho_{\mathbf{k}}(\omega) = -\frac{1}{\pi}\mathrm{Im}\, G_{\mathbf{k},\sigma}(\omega + i\delta)$ as $\epsilon(\mathbf{k})$ is varied, where

$$G_{\mathbf{k},\sigma}(\omega) = \frac{1}{\omega + \mu - \epsilon(\mathbf{k}) - \Sigma_\sigma(\omega)}$$

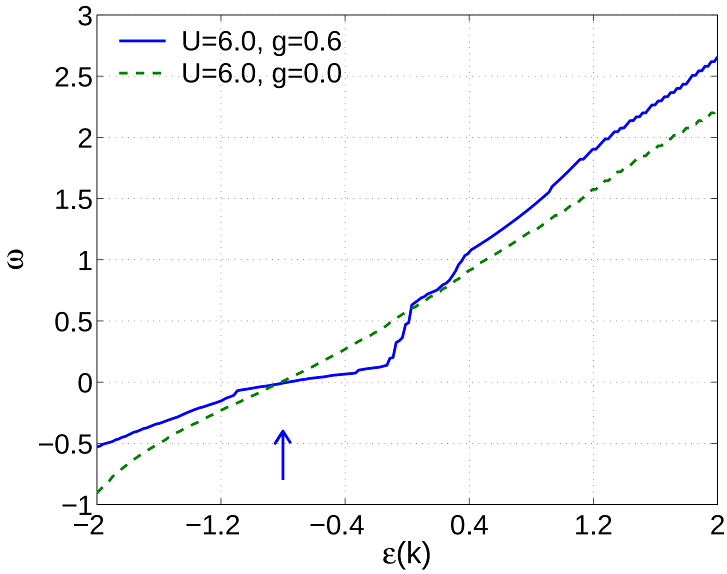

Plot of position of maximimum as a function of $\epsilon(\mathbf{k})$.

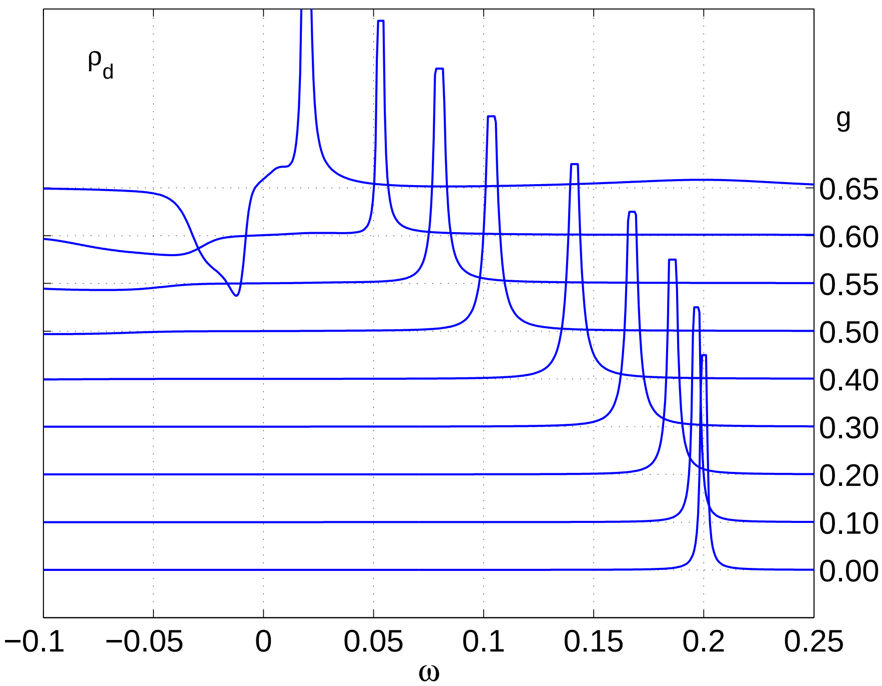

Softening of the phonon spectrum with increasing value of g.

The position of the kink in the quasiparticle dispersion correlates with the renormalised phonon frequency.

Luttinger's Theorem

Fermi surface of non-interacting system:

$$\epsilon(\mathbf{k}_{\rm F}) = \mu_0$$

Fermi surface of interacting system:

$$\epsilon(\mathbf{k}_{\rm F}) = \mu - \Sigma(0),$$

For same number of particles:

$$\mu_0 = \mu - \Sigma(0),$$

We can check the theorem by calculating n, in two ways:

(i) From $\mu_0 = \mu - \Sigma(0)$ we can calculate n from the volume of the non-interacting Fermi surface.

(ii) We can deduce n from the expectation value $\langle n_i \rangle$ from the ground state of the interacting system.

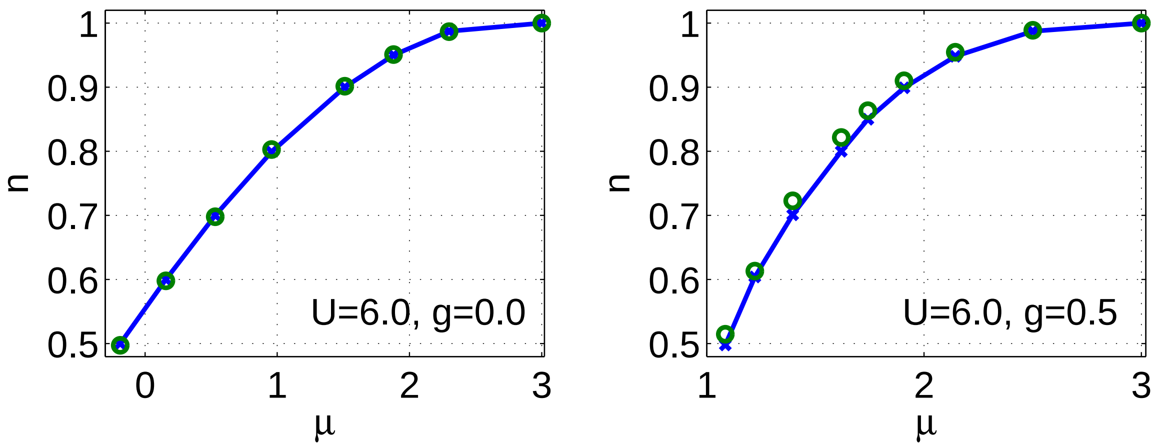

From (i)-circles and from (ii) full lines.

Polaronic Quasiparticle Band

Expanding the self-energy about the Fermi level, $\omega = 0$, the retaining only the first two terms, $\Sigma(0) + \omega\Sigma'(0)$,

$$\tilde{G}_{\mathbf{k},\sigma}(\omega) = \frac{1}{\omega + \tilde{\mu} - \tilde{\epsilon}(\mathbf{k})}$$

where $\tilde{\epsilon}(\mathbf{k}) = z\epsilon(\mathbf{k})$, and z is the usual wavefunction renormalization factor $z = (1 - \Sigma'(0))^{-1}$, and $\tilde{\mu} = z(\mu - \Sigma(0))$ is a renormalized chemical potential.

The corresponding density of states $\tilde{\rho}_0(\omega)$ for the non-interacting quasiparticles is given by

$$\tilde{\rho}_0(\omega) = \frac{2}{\pi \tilde{D}^2}\sqrt{\tilde{D}^2 - (\omega + \tilde{\mu})^2}$$

where $\tilde{D} = zD$ plays the role of a renormalized band width. Luttinger's theorem is satisfied as $\tilde{\mu} = z\mu_0 = z(\mu - \Sigma(0))$ and the interacting and quasiparticle Fermi surface $(\tilde{\epsilon}(\mathbf{k}) = \tilde{\mu})$ is the same as that of the non-interacting system.

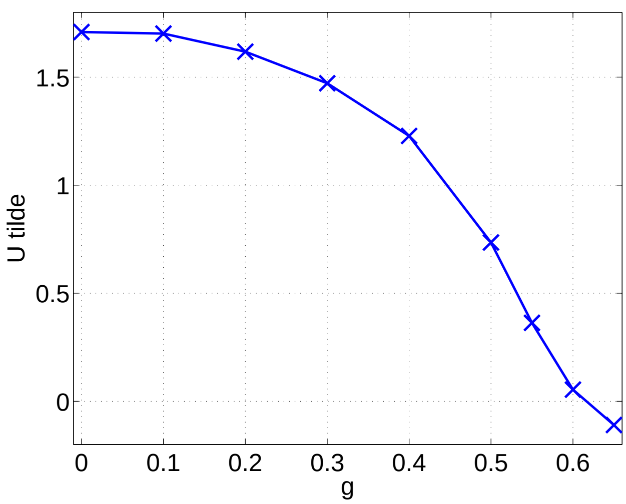

Renormalised interaction $\tilde{U}$ between the quasiparticles.

Fermi Liquid Theory and the Anderson Model

Quasiparticles in the Anderson model:

$$H_{\rm AM} = \sum_\sigma \epsilon_d d^\dagger_\sigma d_\sigma + U n_{d,\uparrow} n_{d,\downarrow} + \sum_{k,\sigma} (V_k d^\dagger_\sigma c_{k,\sigma} + V_k{}^* c^\dagger_{k,\sigma} d_\sigma) + \sum_{k,\sigma} \epsilon_{k,\sigma} c^\dagger_{k,\sigma} c_{k,\sigma},$$

energy of the impurity level ϵ_d, interaction at the impurity site U, hybridization matrix element V_k, conduction electron energy ϵ_k.

$$G_d(\omega) = \frac{1}{\omega - \epsilon_d - V^2 g_0(\omega) + \Sigma(\omega)}$$

where $g_0(\omega) = -i\pi\rho_0$ for a wide conduction band, so

$$G_d(\omega) = \frac{1}{\omega - \epsilon_d + i\Delta + \Sigma(\omega)}$$

where $\Delta = iV^2 g_0(\omega) = \pi\rho_0 V^2$.
We expand $\Sigma(\omega) = \Sigma(0) + \omega\Sigma'(0) + ...$

$$G_d(\omega) = \frac{z}{\omega - \tilde\epsilon_d + i\tilde\Delta}$$

where

$$\tilde\epsilon_d = z(\epsilon_d + \Sigma(0)) \qquad \tilde\Delta = z\Delta$$

and $z = 1/(1 - \Sigma'(0))$. Rescale the fields so that

$$\tilde G_d(\omega) = \frac{1}{\omega - \tilde\epsilon_d + i\tilde\Delta}$$

so this is the quasiparticle Green's function corresponding to a renormalized non-interacting Anderson model.

Calculation of $\tilde{\epsilon}_d$ and $\tilde{\Delta}$ using the NRG

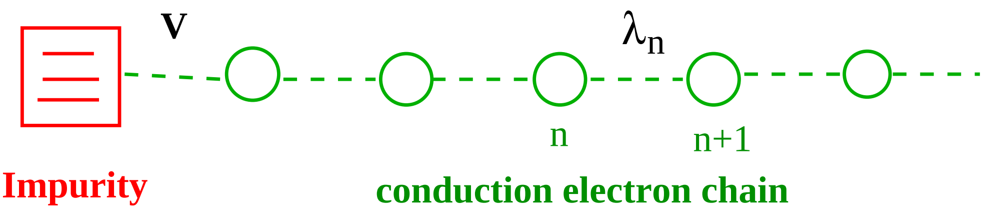

Given an ϵ_d and hybridization V, the one-particle excitations $\omega = \epsilon_n$ are given by the poles of

$$G_d^{(0)}(\omega) = \frac{1}{\omega - \epsilon_d - V^2 g_0(\omega)}$$

ie, solutions of

$$\omega - \epsilon_d - V^2 g_0(\omega) = 0$$

In the inverse case, given the solutions ϵ_n, we can use this equation to deduce the parameters ϵ_d and V. We can apply this to the NRG results.

If $E_p(N)$, $E_h(N)$ are the lowest energy single particle excitations of the interacting Anderson model, then from the equation

$$\omega\Lambda^{-(N-1)/2} - \tilde{\epsilon}_d(N) = \Lambda^{(N-1)/2}\tilde{V}(N)^2 g_0(\omega),$$

we can deduce the effective parameters, $\tilde{\epsilon}_d(N)$ and $\tilde{\Delta}(N) = \pi\tilde{V}(N)^2/D$. If these can be described by a non-interacting Anderson model, then they should be independent of N.

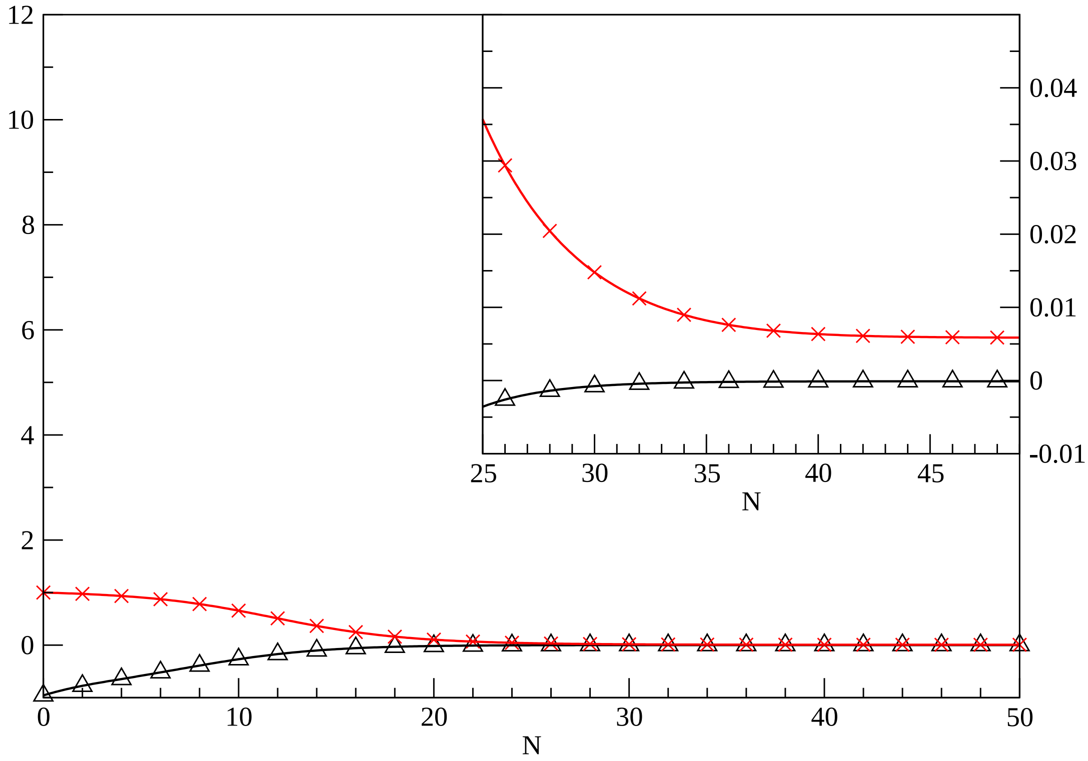

The colour **black** curve is the value of $\tilde{\epsilon}_d(N)$.

The colour red curve is the value of $\tilde{\Delta}(N) = \pi\tilde{V}(N)^2/D$.

The values of the 'bare' parameters are $\pi\Delta = 0.05$, $\epsilon_d = -0.2$, $U = 0.3$.

Quasiparticle Interactions

We can also define a local renormalized interaction $\tilde{U}$

If $E_{pp}(N)$ is the energy of a two-quasiparticle excitation, we can define an N-dependent renormalized interaction $\tilde{U}_{pp}(N)$ via,

$$E_{pp}(N) - 2E_p(N) = \tilde{U}(N)\Lambda^{(N-1)/2}|\psi^*_{p,1}(-1)|^2|\psi^*_{p,1}(-1)|^2,$$

where $|\psi_{p,1}(-1)|^2$ is given by

$$|\psi_{p,1}|^2 = \frac{1}{1 - \tilde{V}^2(N)\Lambda^{(N-1)}g'_0(E_p(N))},$$

Similar equations for $\tilde{U}_{hh}(N)$ and $\tilde{U}_{ph}(N)$

We find a unique limit,

$$\lim_{N\to\infty} \tilde{U}_{pp}(N) = \lim_{N\to\infty} \tilde{U}_{hh}(N) = \lim_{N\to\infty} \tilde{U}_{ph}(N) = \tilde{U}$$

We can define a quasiparticle density of states:

$$\tilde{\rho}(\omega) = \frac{\tilde{\Delta}/\pi}{(\omega - \tilde{\epsilon}_d)^2 + \tilde{\Delta}^2}$$

For strong coupling it can be shown that

$$\tilde{U}\tilde{\rho}(0) \to 1$$

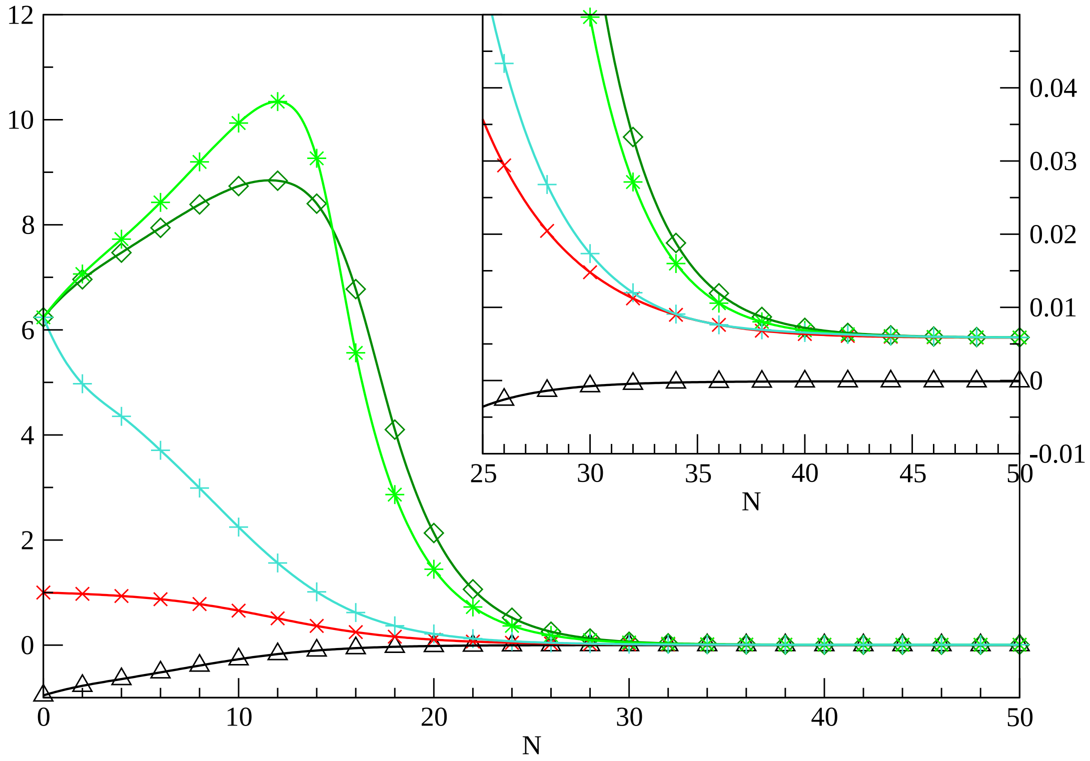

The colour **black** curve is the value of $\tilde{\epsilon}_d(N)$.

The colour red curve is the value of $\tilde{\Delta}(N) = \pi\tilde{V}(N)^2/D$.

The colour green and turquoise curves give the values of $\tilde{U}_{pp}$, $\tilde{U}_{hh}$ and $\tilde{U}_{ph}$.

We are in the Kondo regime so there is only one energy scale

$$\tilde{U} = \pi\tilde{\Delta} = 4T_{\rm K}$$

.

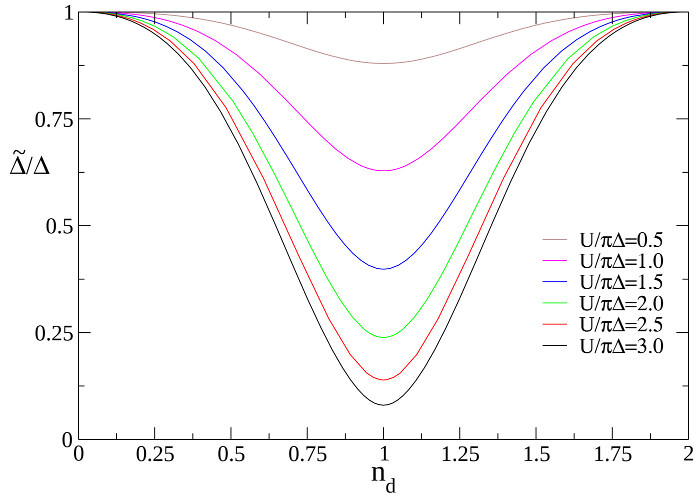

$U > 0$: Gives wavefunction renormalization factor $z = \tilde{\Delta}/\Delta$ (quasiparticle weight) as a function of filling n_d. The maximum renormalization is at half-filling giving the minimum value of z.

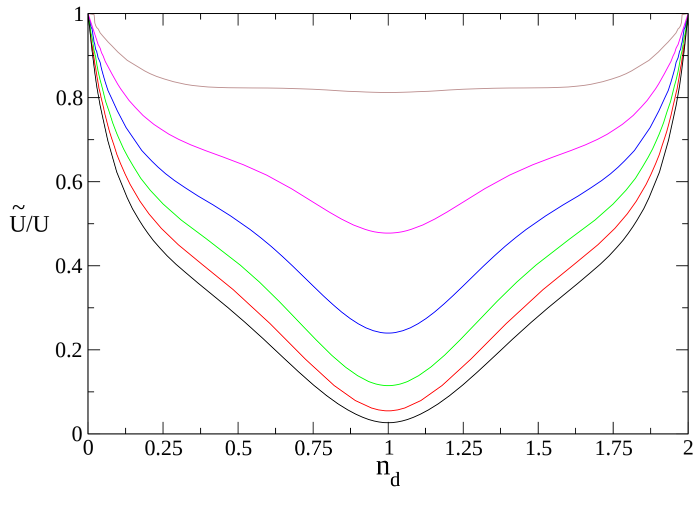

The ratio of the quasiparticle interaction $\tilde{U}$ to the bare interaction U as a function of filling n_d. The minimum value of $\tilde{U}$is at half-filling rising to the bare value at $n_d = 0$ and $n_d = 1$.

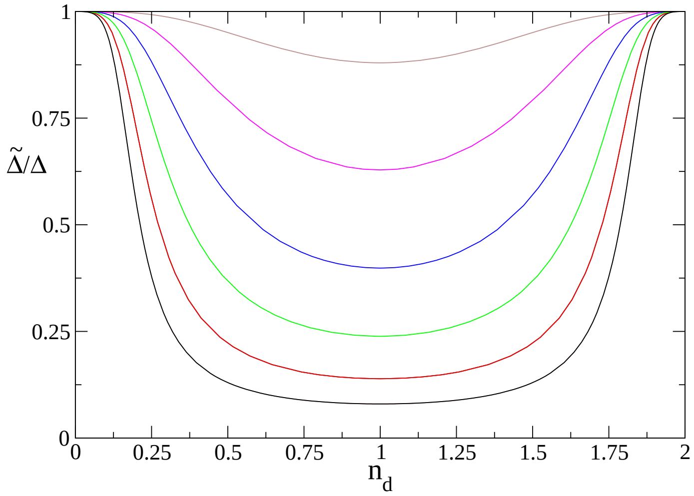

$U < 0$: z is flat as a function of n_d for a broad range near $n_d \sim 1$.

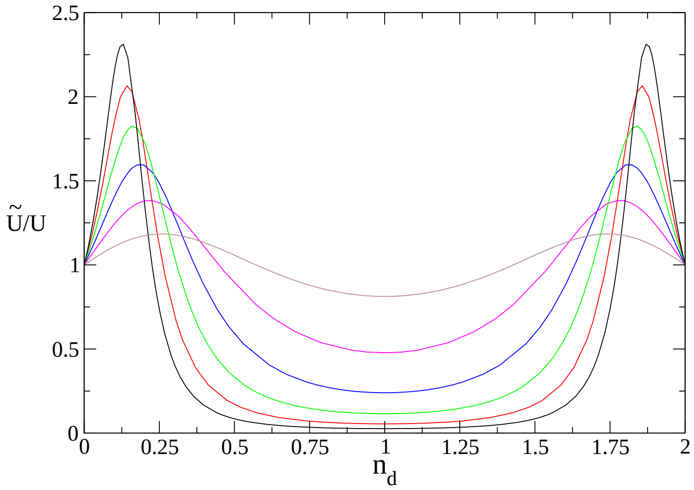

$\tilde{U}$ is also flat as a function of n_d for a broad range near $n_d \sim 1$. In contrast to the case with $U > 0$ there is a range where $|\tilde{U}| > |U|$ before it approaches the bare value at $n_d = 0$ and $n_d = 1$.

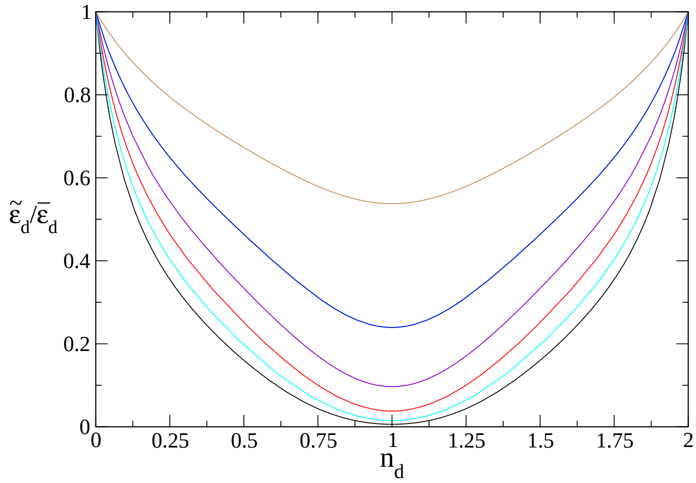

$U < 0$: Ratio $\tilde{\epsilon}_d/\bar{\epsilon}_d$, where $\bar{\epsilon}_d = \epsilon_d + U/2$, is always < 1.

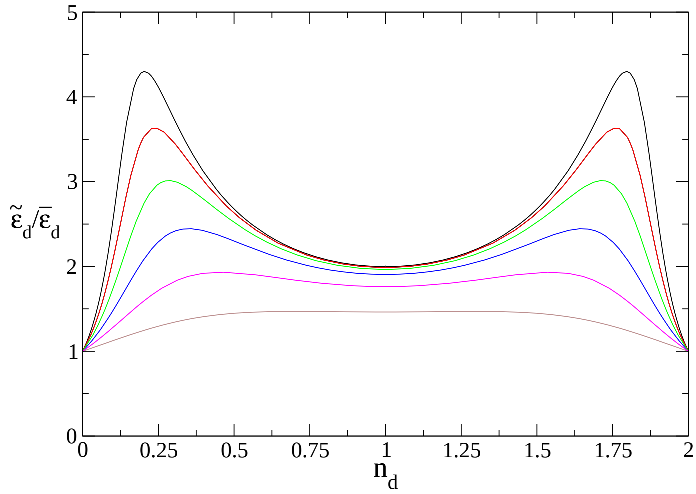

$U < 0$: Ratio $\tilde{\epsilon}_d/\bar{\epsilon}_d$ is always > 1 and has maxima as $n_d \rightarrow 0$ and $n_d \rightarrow 1$.

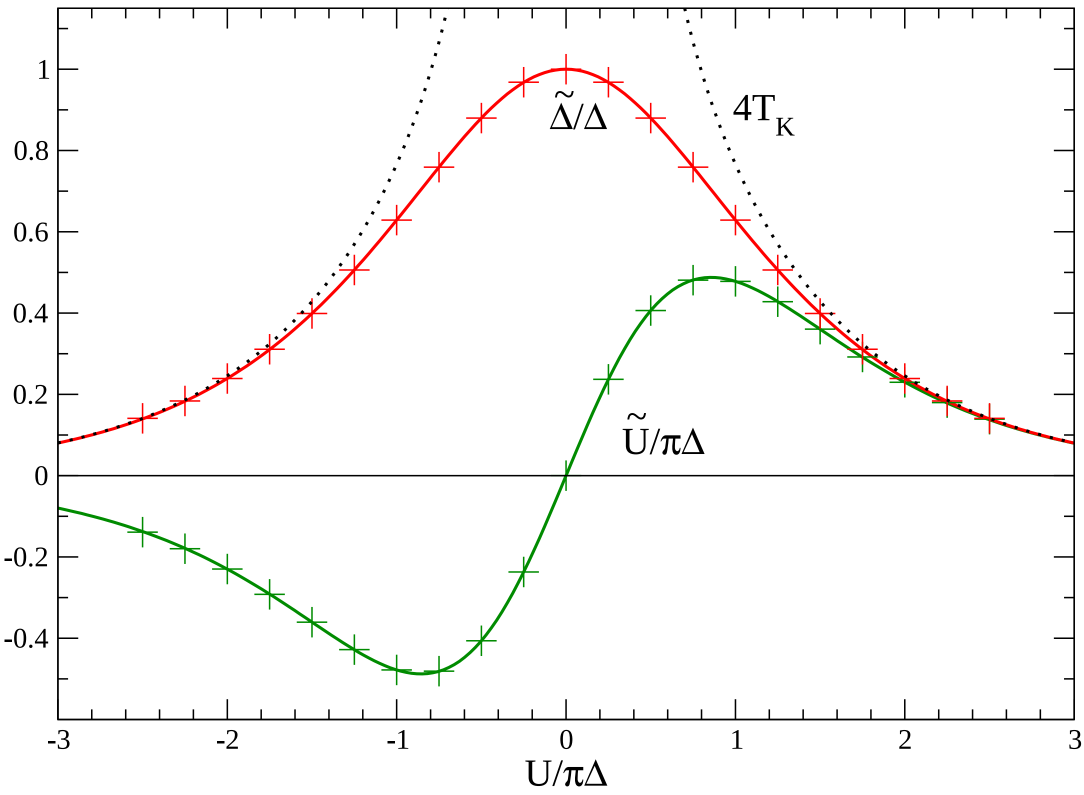

This plot shows how the renormalized parameters vary as the value of U varies for the symmetric model $\epsilon_d = -U/2$.

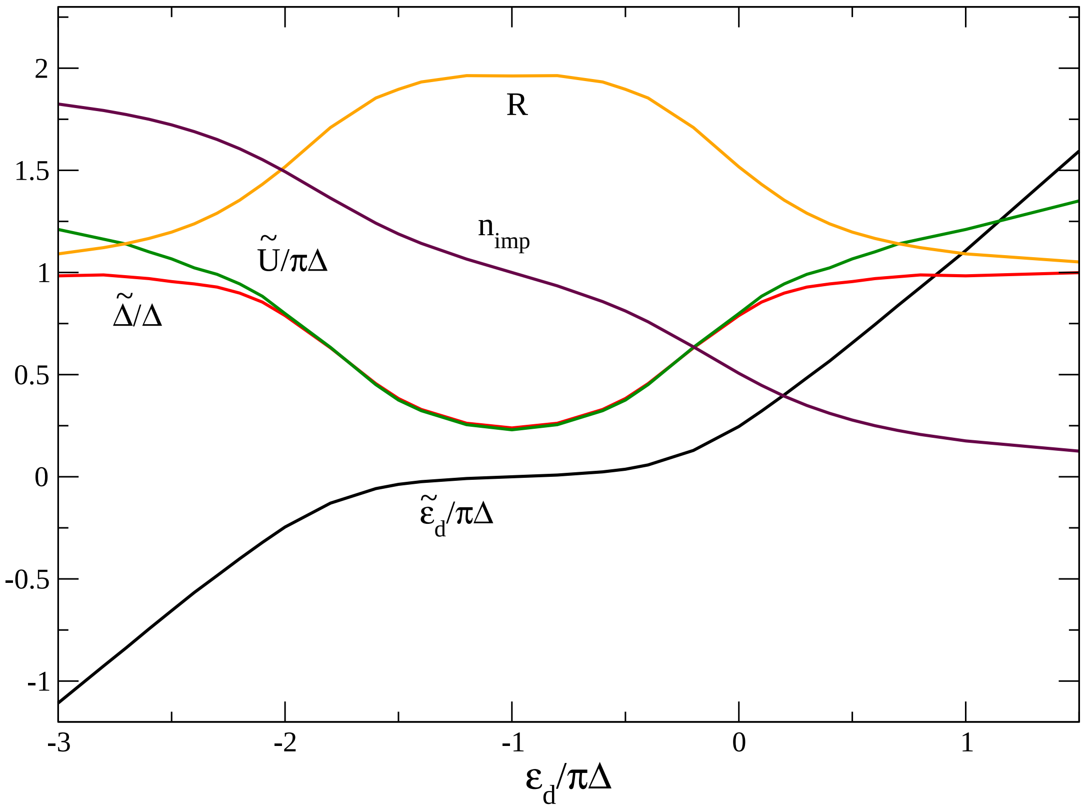

This plot shows how the renormalized parameters vary as the impurity level is moved from well below the Fermi level to well above for a fixed value of $U = 2\pi\Delta$.

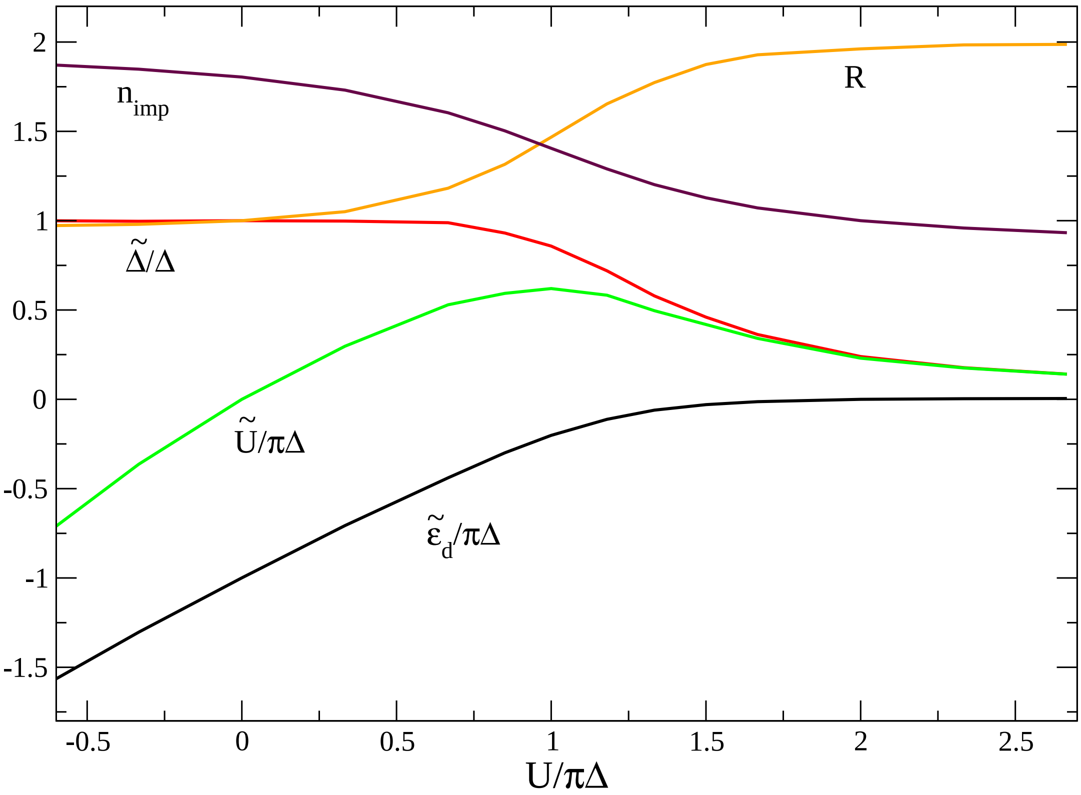

This plot shows how the renormalized parameters vary as U varies for a fixed impurity level $\epsilon_d = \pi\Delta$.

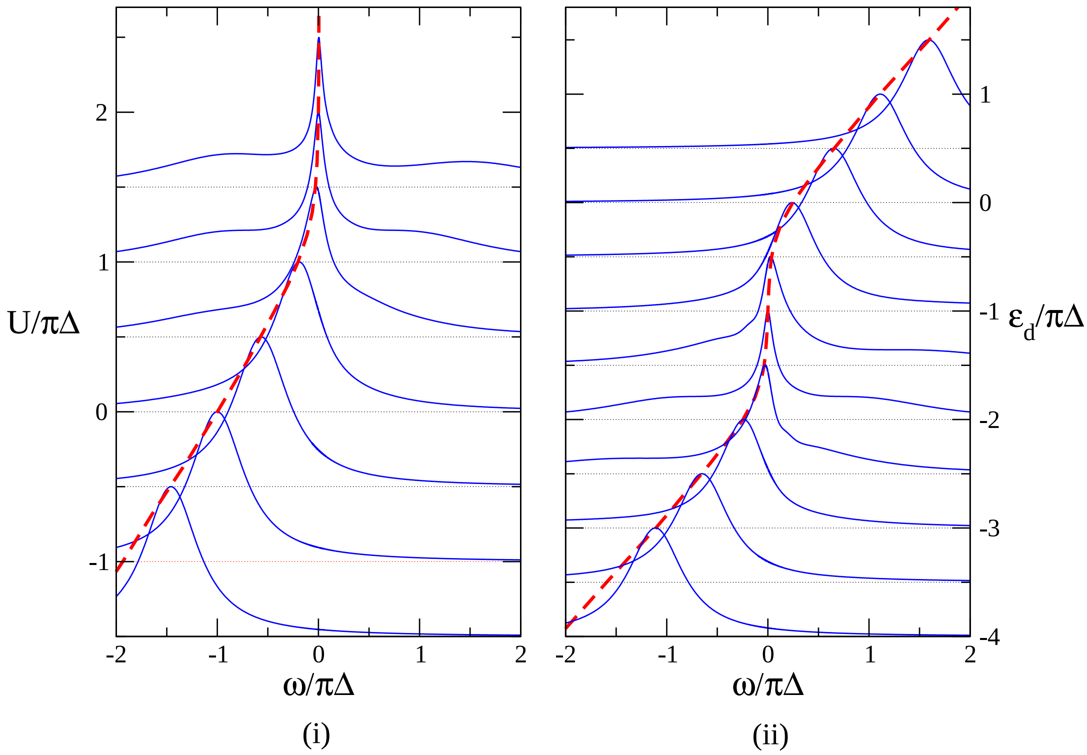

This plot shows how the position of the renormalized level relates to the peaks in the spectral density of the impurity Green's function, for the two cases presented.

Renormalized Perturbation Theory for the Anderson Model

No divergences associated with lack of cut-off in this case.

$$G_d(\omega) = \frac{1}{\omega - \epsilon_d + i\Delta + \Sigma(\omega)}$$

We eliminate $\Sigma(0)$ and $\Sigma'(0)$ explicitly,

$$\Sigma(\omega) = \Sigma(0) + \omega\Sigma'(0) + \Sigma^{\rm rem}(\omega)$$

$$G_d(\omega) = \frac{z}{\omega - \tilde{\epsilon}_d + i\tilde{\Delta} + \tilde{\Sigma}(\omega)}$$

where

$$\tilde{\epsilon}_d = z(\epsilon_d + \Sigma(0)) \qquad \tilde{\Delta} = z\Delta \qquad \tilde{\Sigma}(\omega) = z\Sigma^{\rm rem}(\omega)$$

and $z = 1/(1 - \Sigma'(0))$.

Rescale the fields so that

$$\tilde{G}_d(\omega) = \frac{1}{\omega - \tilde{\epsilon}_d + i\tilde{\Delta} + \tilde{\Sigma}(\omega)}$$

U is replaced by the renormalized one,

$$\tilde{U} = z^2\Gamma_{\uparrow,\downarrow}(0,0,0,0)$$

We have used the Luttinger result ${\rm Im}\Sigma'(0) = 0$.

Renormalized Perturbation Theory

$$\mathcal{L}(\epsilon_d, \Delta, U) = \mathcal{L}(\tilde{\epsilon}_d, \tilde{\Delta}, \tilde{U}) + \mathcal{L}^{\rm counter}(\lambda_1, \lambda_2, \lambda_3)$$

The expansion is carried out in powers of $\tilde{U}$, with $\lambda_1, \lambda_2, \lambda_3$ determined by the renormalization conditions:

(i) $\tilde{\Sigma}(0) = 0$

(ii) $\tilde{\Sigma}'(0) = 0$

(iii) $\tilde{\Gamma}_{\uparrow,\downarrow}(0,0,0,0) = \tilde{U}$

Renormalizability is not an issue because we have no ultraviolet divergences due to a lack of an upper cut-off.

Note that the renormalized form of $\mathcal{L}$ is the same as that of the original so the corresponding Hamiltonian is simply a renormalized version of the Anderson model. i.e. $\epsilon_d \to \tilde{\epsilon}_d$, $\Delta \to \tilde{\Delta}$ and $U \to \tilde{U}$.

Low order results are asymptotically exact as $T \to 0$

All the leading order **exact** low temperature results, which correspond to a local Fermi liquid theory, can be calculated by working to **second order** in $\tilde{U}$ only.

Zero Order

$$n_{\mathrm{d},\sigma} = \tilde{n}_{\mathrm{d},\sigma} = \frac{1}{2} - \frac{1}{\pi}\tan^{-1}\left(\frac{\tilde{\epsilon}_{\mathrm{d},\sigma}}{\tilde{\Delta}}\right)$$

and

$$\gamma_{\mathrm{imp}} = \frac{2\pi^2}{3}\tilde{\rho}(0) \quad \text{with} \quad \tilde{\rho}(0) = \frac{\tilde{\Delta}/\pi}{\tilde{\epsilon}_d^2 + \tilde{\Delta}^2}$$

First Order

$$\chi_{\mathrm{imp}} = \frac{(g\mu_{\mathrm{B}})^2}{2}\tilde{\rho}(0)(1+\tilde{U}\tilde{\rho}(0)), \quad \chi_{\mathrm{c,imp}} = 2\tilde{\rho}(0)(1-\tilde{U}\tilde{\rho}(0))$$

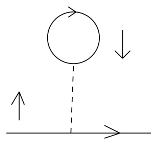

Second Order

$$\sigma_{\mathrm{imp}}(T) = \sigma_0\left\{1 + \frac{\pi^2}{3}\left(\frac{T}{\tilde{\Delta}}\right)^2\left(1 + 2\left(\frac{\tilde{U}}{\pi\tilde{\Delta}}\right)^2\right) + \mathrm{O}(T^4)\right\}$$

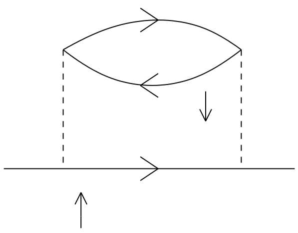

THE KONDO LIMIT—-ONLY ONE RENORMALIZED PARAMETER $\mathrm{T_K}$

In the localized limit, $n_d \to 1$, $\tilde{\epsilon}_d \to 1$ and $\chi_{\rm c,imp} \to 0$,

$$\tilde{U} = \pi\tilde{\Delta} = 4T_{\rm K}$$

$$\gamma_{\rm imp} = \frac{\pi^2}{6T_{\rm K}} \qquad \chi_{\rm imp} = \frac{(g\mu_{\rm B})^2}{4T_{\rm K}}$$

$$\sigma_{\rm imp}(T) = \sigma_0\left\{1 + \frac{\pi^2}{16}\left(\frac{T}{T_{\rm K}}\right)^2 + {\rm O}(T^4)\right\}$$

N-fold Degenerate Anderson Model

$$\tilde{\Delta} = T_{\rm K}\frac{N^2{\rm sin}^2(\pi/N)}{\pi(N-1)} \qquad \tilde{\epsilon}_d = T_{\rm K}\frac{N^2{\rm sin}(2\pi/N)}{2\pi(N-1)}$$

$$\tilde{U} = T_{\rm K}\left(\frac{N}{N-1}\right)^2$$

The n-Channel Anderson Model with n=2S

$$\tilde{U} = \pi\tilde{\Delta} = 4T_{\rm K} \qquad \tilde{J} = -\frac{8}{3}T_{\rm K}$$

In all cases $T_{\rm K}$ is defined such that $\chi_{\rm imp} = (g\mu_{\rm B})^2 S(S+1)/3T_{\rm K}$.

Quasiparticles in the limit $z \to 0$

If $U \to \infty$ which corresponds to $z \to 0$,

$$\tilde{\Delta} \to 4T_{\rm K}/\pi \to 0$$

$$\tilde{\epsilon}_f \to 0$$

and

$$\tilde{\rho}(\omega) \to \delta(\omega)$$

but

$$\tilde{U}\rho(0) \to 1$$

Hence, the results for the spin and charge susceptibility at $T = 0$,

$$\chi_{\rm imp} = \frac{(g\mu_{\rm B})^2}{2}\tilde{\rho}(0)(1 + \tilde{U}\tilde{\rho}(0)), \quad \chi_{\rm c,imp} = 2\tilde{\rho}(0)(1 - \tilde{U}\tilde{\rho}(0))$$

in this limit give

$$\chi_{\rm imp} \to \infty, \quad \chi_{\rm c,imp} \to 0$$

What is more if we consider $T \neq 0$ and include the Fermi factors we find

$$\chi_{\rm imp} \to \frac{(g\mu_{\rm B})^2}{4T}, \quad \chi_{\rm c,imp} \to 0$$

The Fermi liquid theory describes a local moment!

The factor $1+\tilde{U}/\pi\tilde{\Delta} \to 2$ ensures the correct Curie constant.

Quasiparticles in a Magnetic Field

We can generalized $\tilde{\epsilon}_{d\sigma}$ $\tilde{\Delta}$ and $\tilde{U}$, such that they become functions of the magnetic field H. Particle-hole symmetric model:

$$\tilde{\epsilon}_{\mathrm{d},\sigma}(h) = z(h)(-h\sigma + \Sigma_\sigma(0,h)), \quad \tilde{\Delta}(h) = z(h)\Delta$$

where $z(h) = 1/(1 - \Sigma'_\uparrow(0,h))$ with $h = g\mu_{\mathrm{B}}H/2$.

The impurity magnetization $M(h)$ at $T = 0$ is then given simply by

$$M(h) = \frac{g\mu_{\mathrm{B}}}{\pi}\tan^{-1}\left(\frac{\tilde{\epsilon}_d(h)}{\tilde{\Delta}(h)}\right)$$

where $\tilde{\epsilon}_d(h) = -\sigma\tilde{\epsilon}_{d\sigma}(h)$.

Exact expression for susceptibility:

$$\tilde{\rho}(\omega,h) = \frac{\tilde{\Delta}(h)}{(\omega - \tilde{\epsilon}_d(h))^2 + \tilde{\Delta}(h)^2}$$

in terms of quasiparticle density of states,

$$\chi_{\mathrm{imp}}(h) = \frac{(g\mu_{\mathrm{B}})^2}{2}\tilde{\rho}(0,h)(1 + \tilde{U}(h)\tilde{\rho}(0,h))$$

We can follow the de-renormalization of the quasiparticles as a function of h.

As $h \to \infty$,

$$\frac{\tilde{\epsilon}_d(h)}{h} \to 1 \quad \tilde{\Delta}(h) \to \Delta \quad \tilde{U}(h) \to U$$

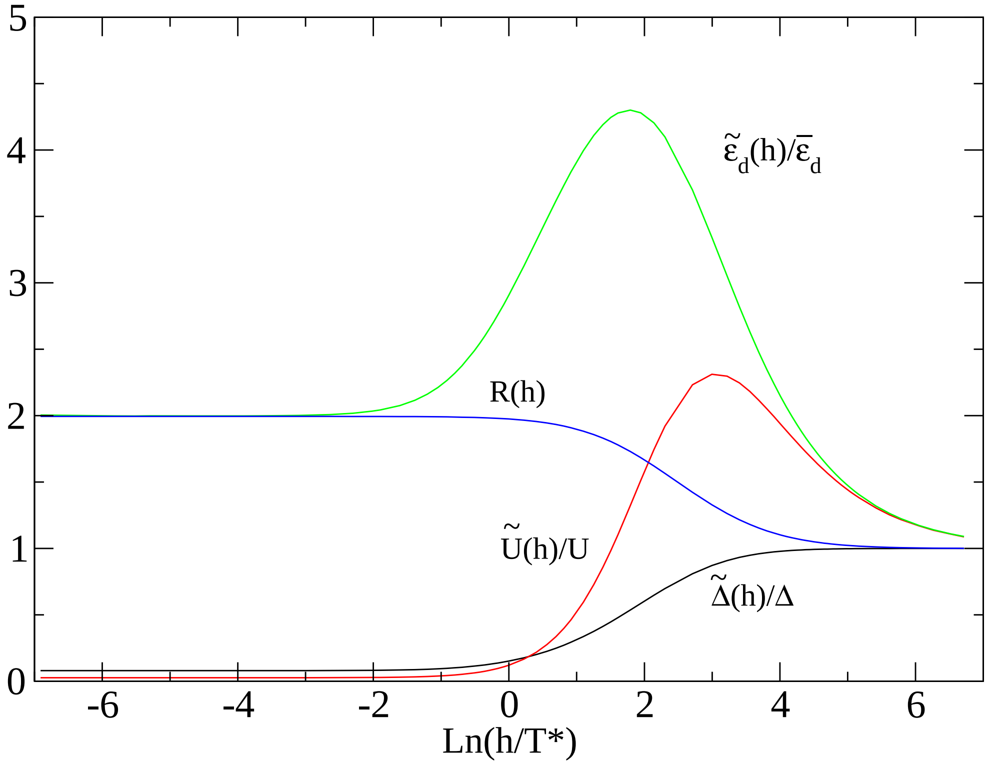

This plot shows how the renormalized parameters vary for the symmetric model at strong coupling ($U/\pi\Delta = 3$) as a function of magnetic field $h = g\mu_B H/2$. The slow derenormalization of the quasiparticles with magnetic field can be seen. $T^* = \pi\tilde{\Delta}/4$ and $T^* \to T_K$ as $U \to \infty$.

The parameters are not independent:

$$1 + \tilde{U}(h)\tilde{\rho}_d(0,h) = \frac{\partial\tilde{\epsilon}_d(h)}{\partial h} - \frac{\tilde{\epsilon}_d(h)}{\tilde{\Delta}(h)}\frac{\partial\tilde{\Delta}(h)}{\partial h}.$$

$\tilde{\epsilon}_d(h) = h + Um_{MF}(h)$, $\tilde{\Delta}(h) = \Delta$, where $m_{MF}(h)$ is the mean field magnetisation. We can deduce the value of $\tilde{U}(h)$ which gives

$$\tilde{U}(h) = \frac{U}{1 - U\tilde{\rho}_{dMF}(0,h)}$$

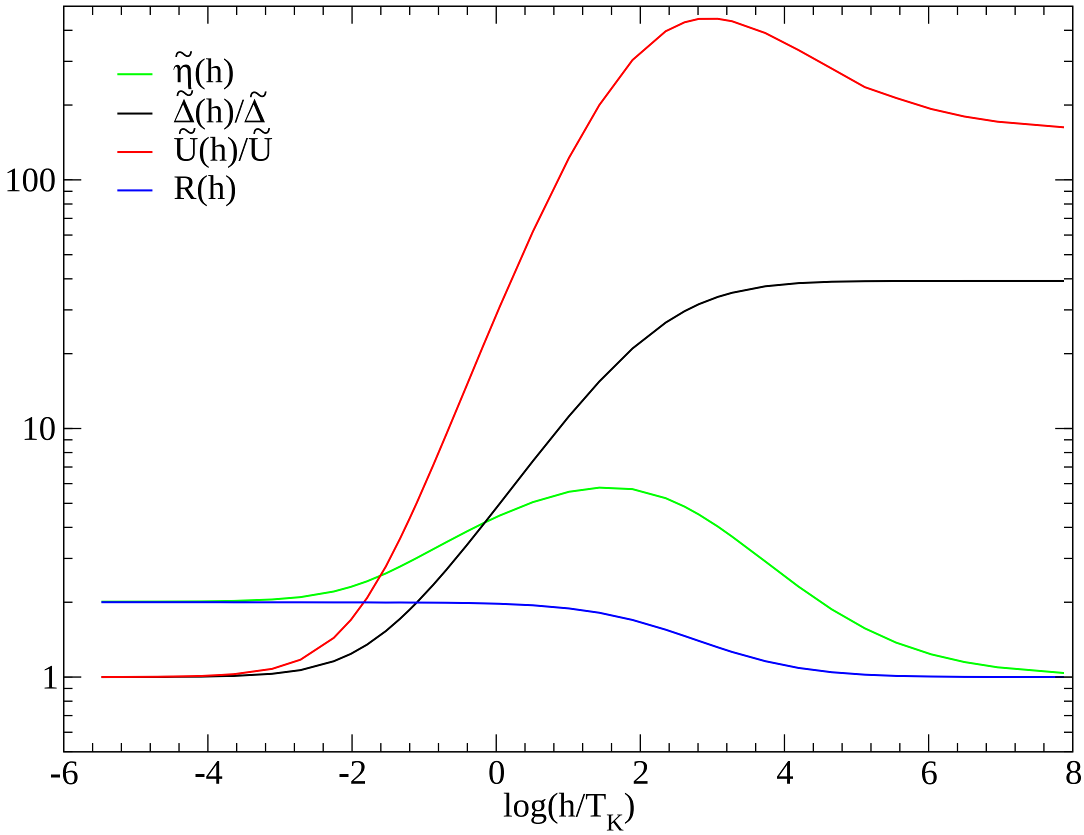

Plot on a logscale of the ratios of the renormalized parameters for h compared to their values at $h = 0$ for $U/\pi\Delta = 4$.

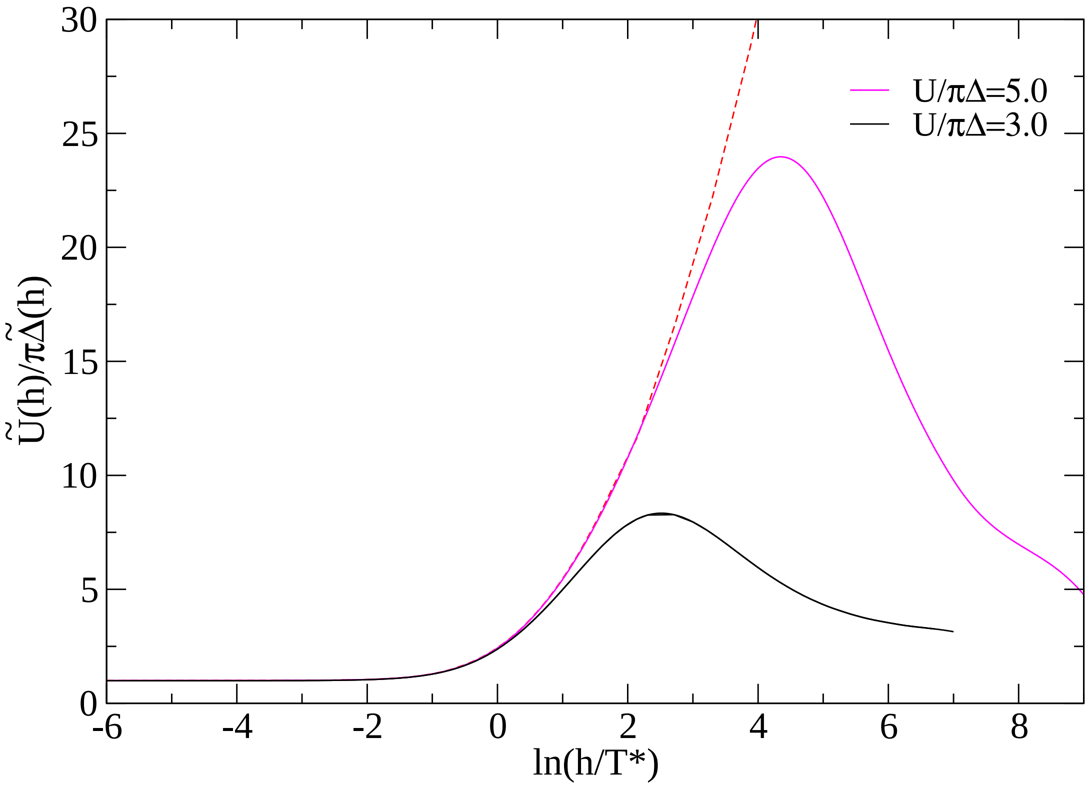

The ratio $\tilde{\epsilon}_{\rm d}(h)/\tilde{\Delta}(h)$ for $U/\pi\Delta = 5.0$ plotted as a function of the logarithm of the magnetic field

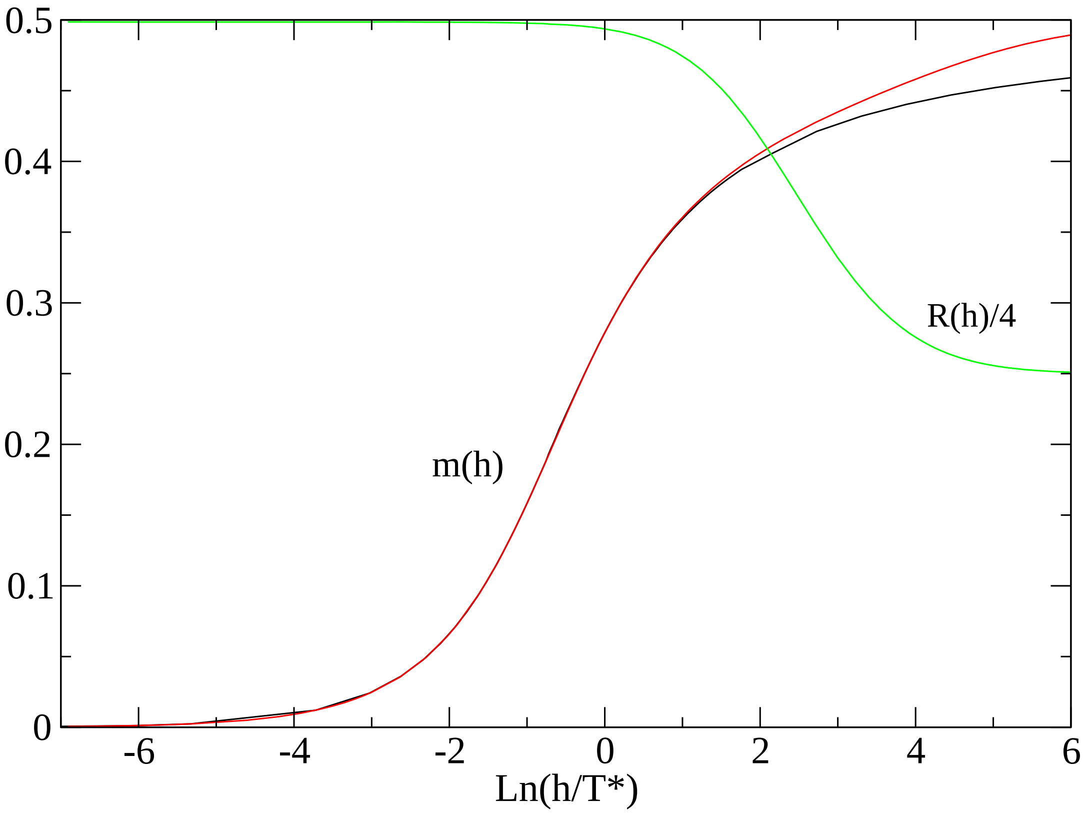

The impurity magnetisation $m(h)$ for the symmetric model with $U/\pi\Delta = 3.0$, together with $R(h)/4$, where $R(h)$ is the Wilson ratio, plotted as a function of the logarithm of the magnetic field. Also shown for comparison are the corresponding Bethe ansatz results for the field induced magnetisation for the Kondo model

$$m(h) = \frac{M(h)}{g\mu_{\rm B}} = \frac{1}{\pi}\tan^{-1}\left(\frac{\tilde{\epsilon}_d(h)}{\tilde{\Delta}(h)}\right)$$

Applications

Susceptibility:

$$\chi_s(0,h) - \chi_s(T,h) = -\frac{\pi^2}{12}T^2\frac{\partial^2 \tilde{\rho}_{\rm d}(0,h)}{\partial h^2} = c_\chi(h)\left(\frac{T}{T^*}\right)^2$$

Impurity contribution to conductivity:

$$\sigma(h,T) = \sigma(h,0)\left\{1 + \sigma_2(h)\left(\frac{\pi T}{\tilde{\Delta}(h)}\right)^2 + {\rm O}(T^4)\right\}$$

Conductance of quantum dot:

$$G(T,h) = G(0,h)\left(1 - G_2(h)\left(\frac{\pi T}{\tilde{\Delta}(h)}\right)^2\right)$$

Differential conductance as a function of V_{ds}:

$$\frac{dI}{dV_{ds}} = G_0(h)\left(1 + A_2(h)V_{ds}^2 + {\rm O}(V_{ds}^4)\right)$$

All have a change of sign of second order term at $h = h_c$,

where h_c lies in the range $0 < h_c < T^*$

Spin and Charge Dynamics

Repeated Quasiparticle Scattering

We look at the contribution from the repeated scattering of a quasiparticle ↑ and a quasihole ↓ to the transverse susceptibility.

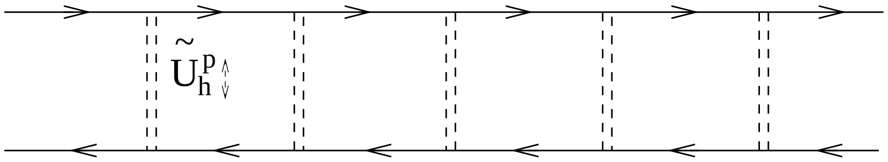

This gives

$$\chi_s(\omega) = \frac{1}{2}\frac{\tilde{\Pi}^{p\uparrow}_{h\downarrow}(\omega)}{1 - \tilde{U}^{p\uparrow}_{h\downarrow}\tilde{\Pi}^{p\uparrow}_{h\downarrow}(\omega)},$$

where $U^{p\uparrow}_{h\downarrow}$ is the irreducible particle-hole vertex.

We determine this from the condition:

$$\chi_s(0) = \frac{1}{2}\frac{\tilde{\rho}(0)}{1 - \tilde{U}^{p\uparrow}_{h\downarrow}\tilde{\rho}(0)} = \frac{\tilde{\rho}(0)}{2}(1 + \tilde{U}\tilde{\rho}(0)),$$

which gives the result,

$$\tilde{U}^{p\uparrow}_{h\downarrow} = \frac{\tilde{U}}{1 + \tilde{U}\tilde{\rho}(0)}$$

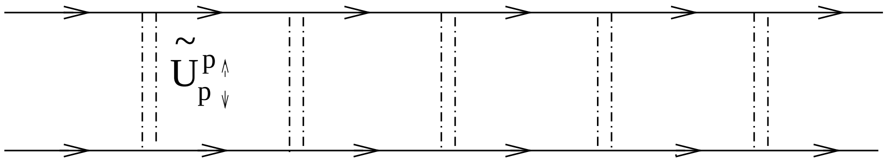

Conributions to the charge susceptibility from repeated scattering of a quasiparticle ↑ and a quasiparticle ↓,

$$\chi_c(\omega) = \frac{1}{2}\frac{\tilde{\Pi}^{p\uparrow}_{p\downarrow}(\omega)}{1-\tilde{U}^{p\uparrow}_{p\downarrow}\tilde{\Pi}^{p\uparrow}_{p\downarrow}(\omega)}$$

where

$$\tilde{U}^{p\uparrow}_{p\downarrow} = \frac{\tilde{U}}{1-\tilde{U}\tilde{\rho}(0)}$$

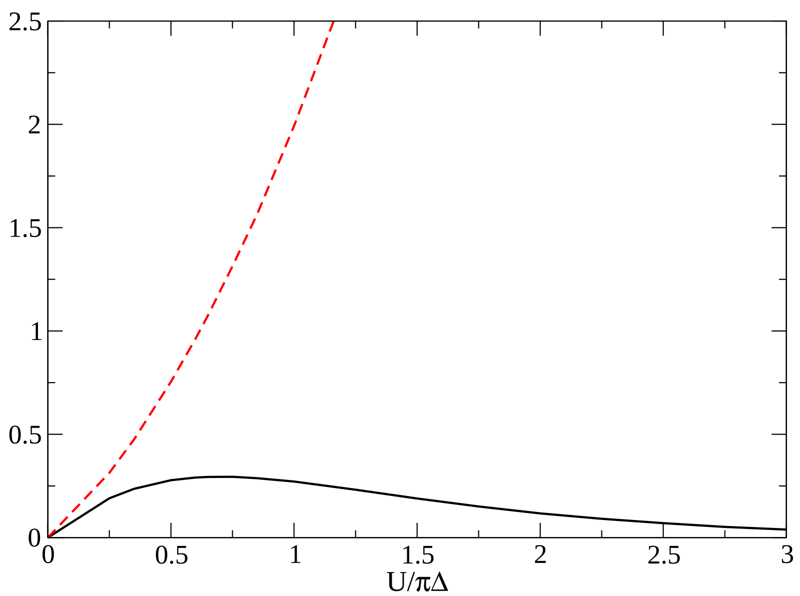

The irreducible vertices, $\tilde{U}^{p\uparrow}_{h\downarrow}$ (black) and $\tilde{U}^{p\uparrow}_{p\downarrow}$ (red) as a function of $U/\pi\Delta$ for the symmetric Anderson model.

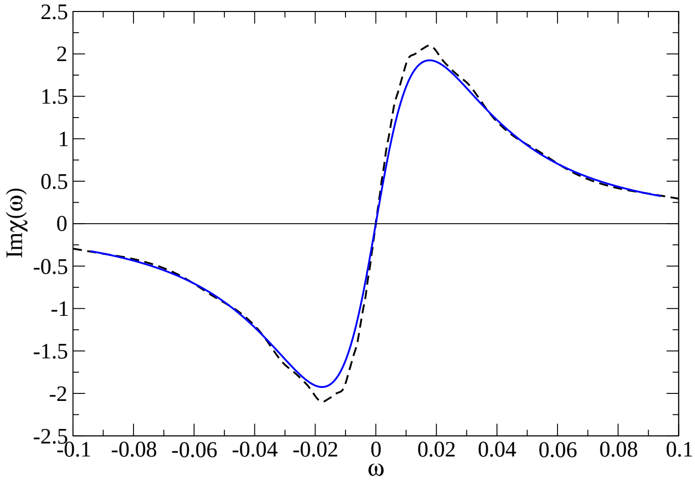

NRG results (black-dashed) for $\mathrm{Im}\,\chi_s(\omega)$ for ($U = 0$) compared with exact results (blue).

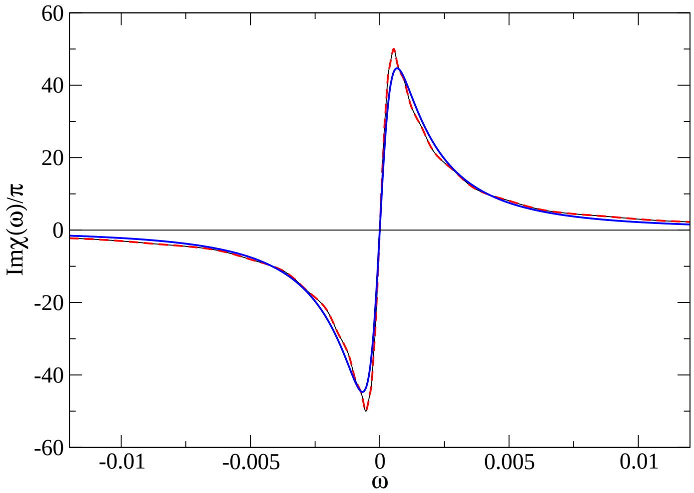

$\mathrm{Im}\,\chi_s(\omega)/\pi$ in the Kondo regime $U/\pi\Delta = 3.0$. The dashed curve (black) is the NRG results and the full line (red) the RPT result.

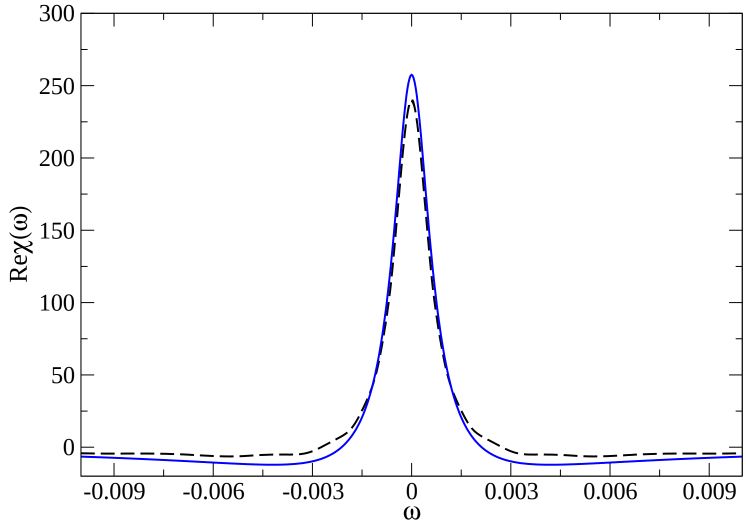

Real part $\chi_s(\omega)$ for the symmetric model in the Kondo regime $U/\pi\Delta = 3.0$. NRG results (black) and RPT (blue).

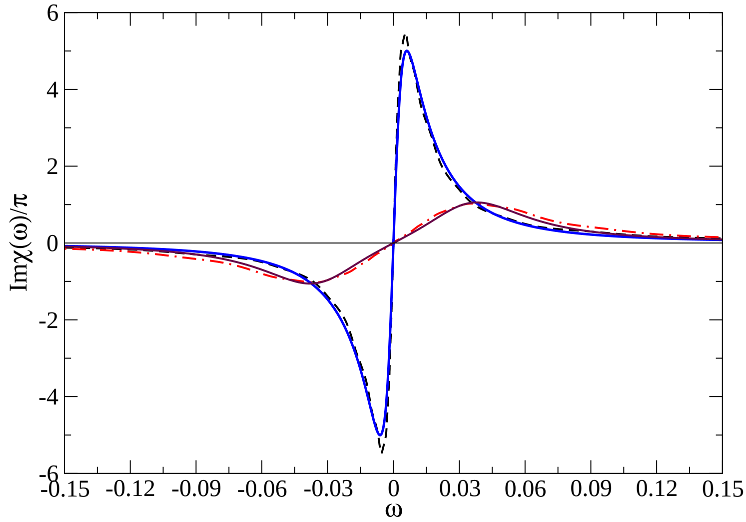

Im$\chi_s(\omega)$ and Im$\chi_c(\omega)$ for $U/\pi\Delta = 1.0$. NRG: spin (black dashed) and charge (black). RPT: spin (blue) and charge (red).

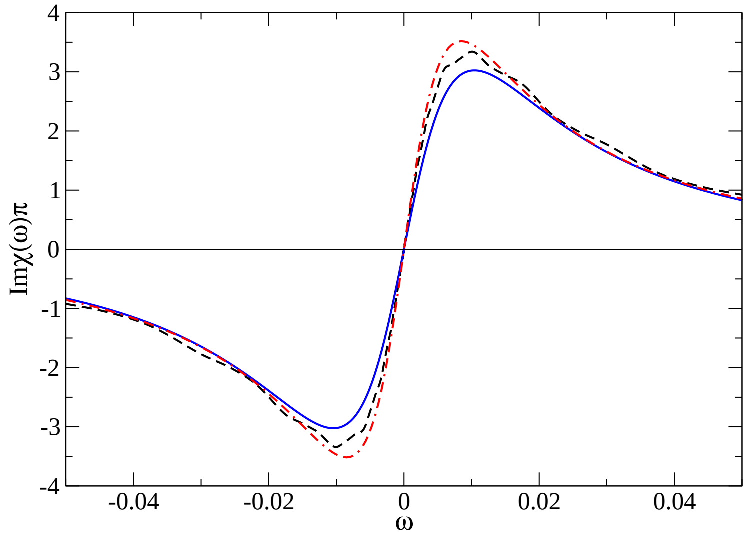

Im $\chi_s(\omega)$ for $U/\pi\Delta = 0.5$. T (i) NRG calculations (black), (ii) RPT (blue) and (iii) RPA (red).

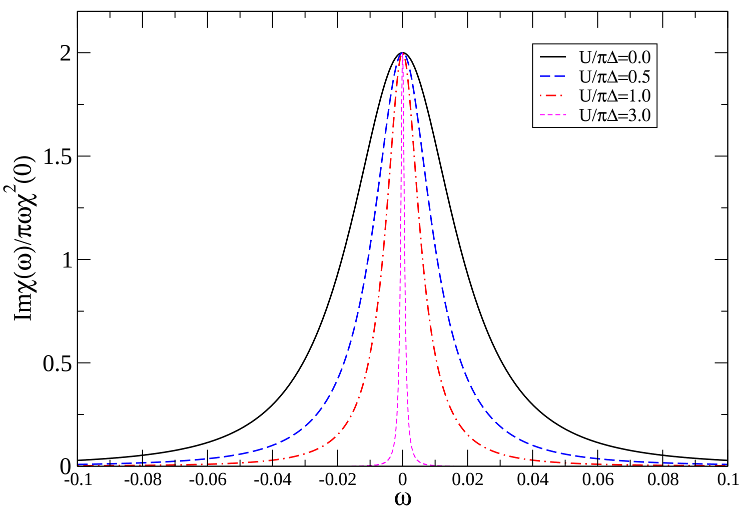

$\mathrm{Im}\chi_s(\omega)/\pi\chi_s^2(0)$ calculated using the RPT for $U/\pi\Delta =$.

$$\text{Area under curve} = \frac{1}{\chi_s(0)} = \frac{2\pi\tilde{\Delta}}{(1+\tilde{U}/\pi\tilde{\Delta})}$$

Spin and Charge Dynamics in a Magnetic Field

$$\chi_{s,\parallel}(0,h) = \frac{1}{2}\tilde{\rho}(0,h)(1+\tilde{U}(h)\tilde{\rho}(0,h))$$

we deduce

$$\tilde{U}^{p\uparrow}_{h\uparrow}(h) = \frac{\tilde{U}(h)}{(1+\tilde{U}(h)\tilde{\rho}(0,h))}$$

$$\chi_{s,\perp}(0,h) = \frac{m(h)}{2h} = \frac{1}{2\pi h}\tan^{-1}\left(\frac{\tilde{h}(h)}{\tilde{\Delta}(h)}\right),$$

we find

$$\tilde{U}^{p\uparrow}_{h\downarrow}(h) = \frac{\pi h(\tilde{\eta}(h)-1)}{\tan^{-1}(\tilde{h}(h)/\tilde{\Delta}(h))}.$$

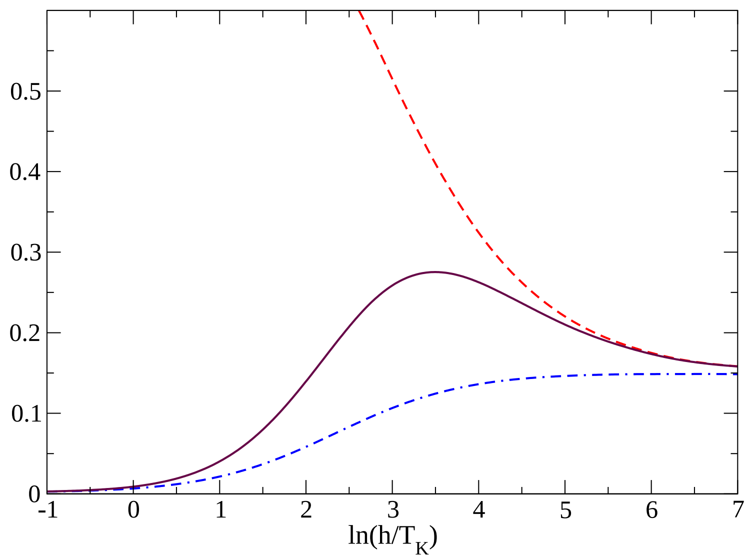

Irreducible vertices, $\tilde{U}^{p\uparrow}_{h\downarrow}(h)$ (black), $\tilde{U}^{p\uparrow}_{h\uparrow}(h)$ (blue), and $\tilde{U}^{p\uparrow}_{p\downarrow}(h)$ (red) as a function of $\ln(h/T_{\rm K})$ for $U/\pi\Delta = 3.0$.

Non-interacting Case $U = 0$

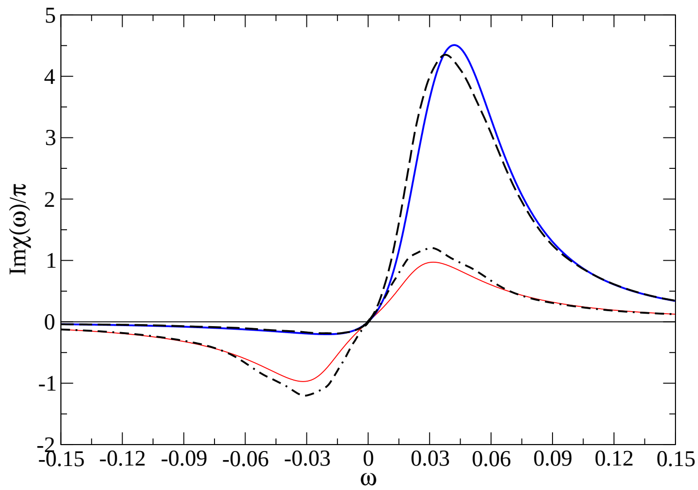

Exact results for $\operatorname{Im}\chi_{s,\perp}(\omega, h)$ (blue) and $\operatorname{Im}\chi_{s,\|}(\omega, h)$ (red) for $U = 0$ compared with the NRG results (black) for $h = 0.4\pi\Delta$.

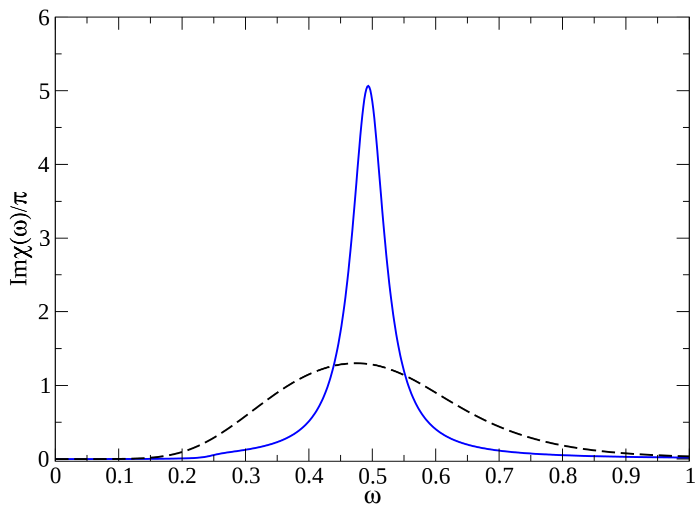

$\operatorname{Im}\chi_{s,\perp}(\omega, h)$ for$U = 0$; NRG (black) and exact results (blue) for $h = 5\pi\Delta$.

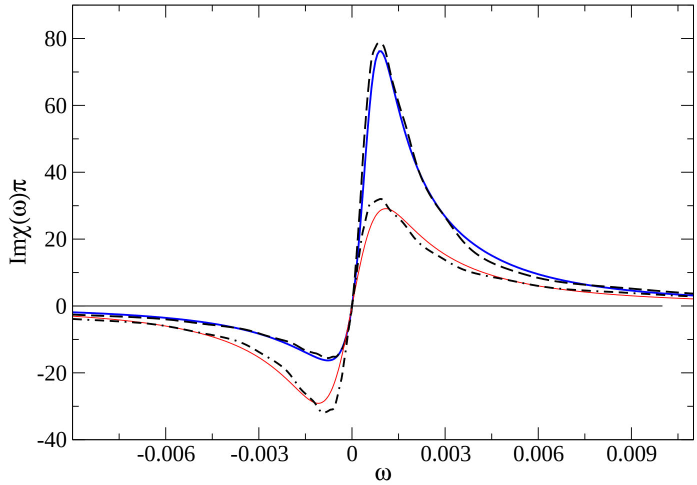

The RPT results for $\mathrm{Im}\,\chi_{s,\perp}(\omega,h)$ (blue) and $\mathrm{Im}\,\chi_{s,\parallel}(\omega,h)$ (red) for $h = 0.4T_{\rm K}$ for $U/\pi\Delta = 3.0$ compared with the NRG results (black).

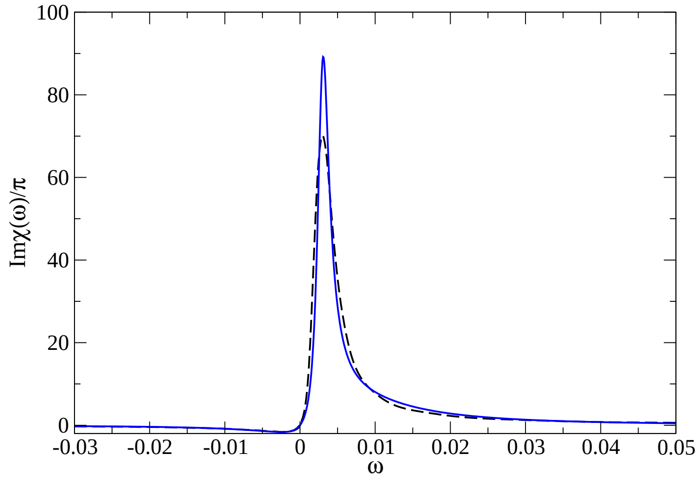

The RPT results for $\mathrm{Im}\,\chi_{s,\perp}(\omega,h)$ (blue) for $h = 2T_{\rm K}$ for $U/\pi\Delta = 3.0$ compared with the NRG results (black).

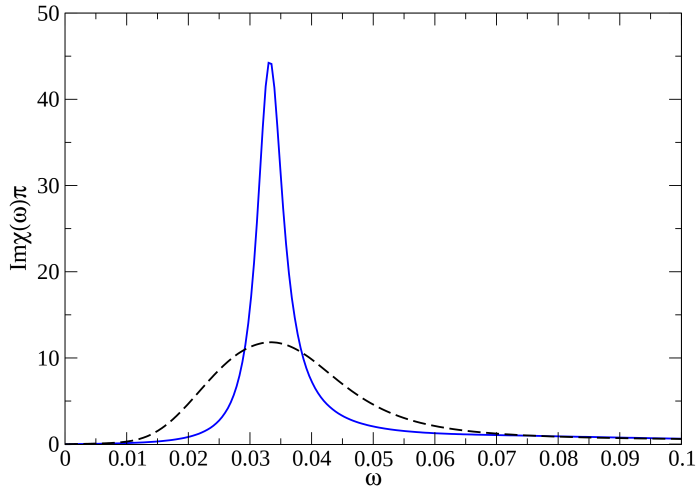

The RPT results (blue) for $\mathrm{Im}\,\chi_{s,\perp}(\omega,h)$ for $h = 20T_{\rm K}$, $(\ln h/T_{\rm K} = 3.0)$ for $U/\pi\Delta = 3.0$ compared with the NRG (black).

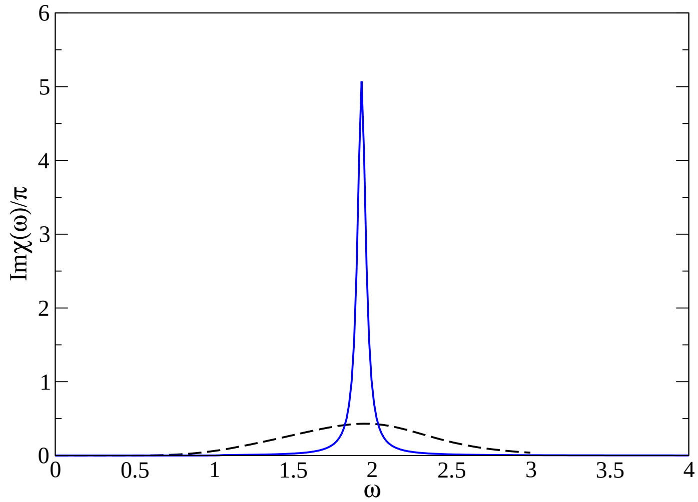

The RPT results for the imaginary parts of $\chi_{s,\perp}(\omega,h)$ (blue) for $h = 10^3T_{\rm K}$ $(\ln h/T_{\rm K} = 6.93)$ as a function of ω for $U/\pi\Delta = 3.0$ compared with the NRG results (black).

In this regime the peak is at $\omega_p = 2h$, and all many-body effects have disappeared.

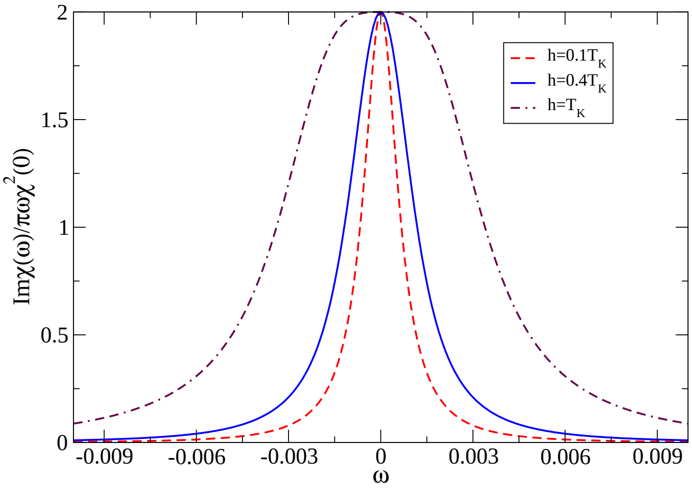

Results for $\mathrm{Im}\chi_{s,\|}(\omega,h)/\pi\chi^2_{s,\|}(0,h)$ calculated using the RPT equations for a range of values of the magnetic field h. The Shiba-Korringa relation for the parallel susceptibility is satisfied in a magnetic field. The area under the curve is equal to $1/\chi_{\|}(h)$, and increases indefinitely as $h \to \infty$.

Contribution to Self-energy from Scattering with Spin Fluctuations

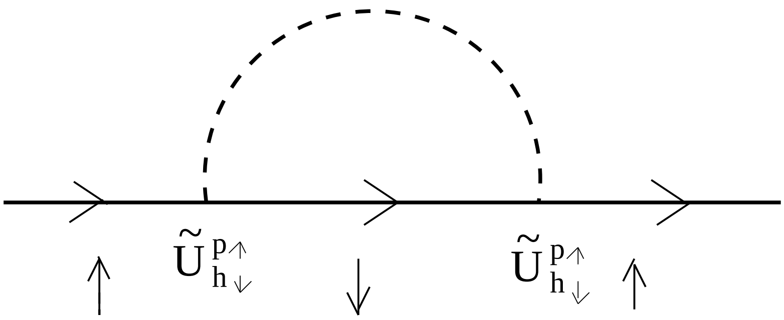

Dashed line is $\chi_{perp}(\omega,h)$. Exact to order ω^2.

$$\rho(\omega,h) = \frac{\tilde{\Delta}}{\Delta}\tilde{\rho}(\omega,h)$$

agrees well with lowest energy peak as a function of h from NRG calculations,

Lattice Case in Dynamical Mean Field Theory

Hubbard Model at half-filling :

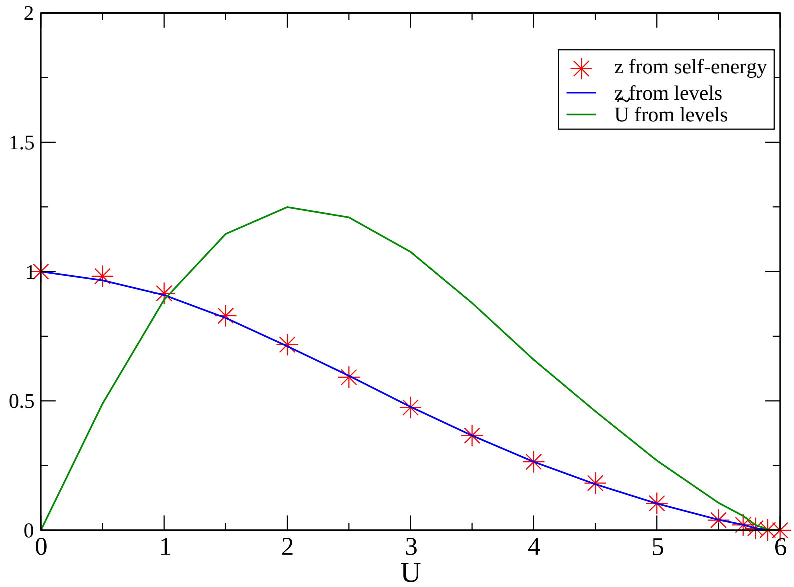

Complete agreement with z calculated from the self-energy and from the renormalized parameters. $\tilde{U}$ does not monotonically increase with U. Ratio $\tilde{U}\tilde{\rho}(0) \rightarrow 0.84$ as $U \rightarrow U_c$

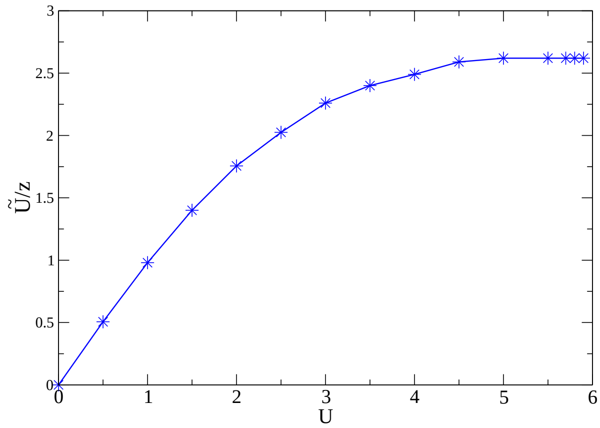

Unique energy scale in strong coupling limit.

Lattice Case in Dynamical Mean Field Theory

Hubbard Model with increasing doping $U = 6$:

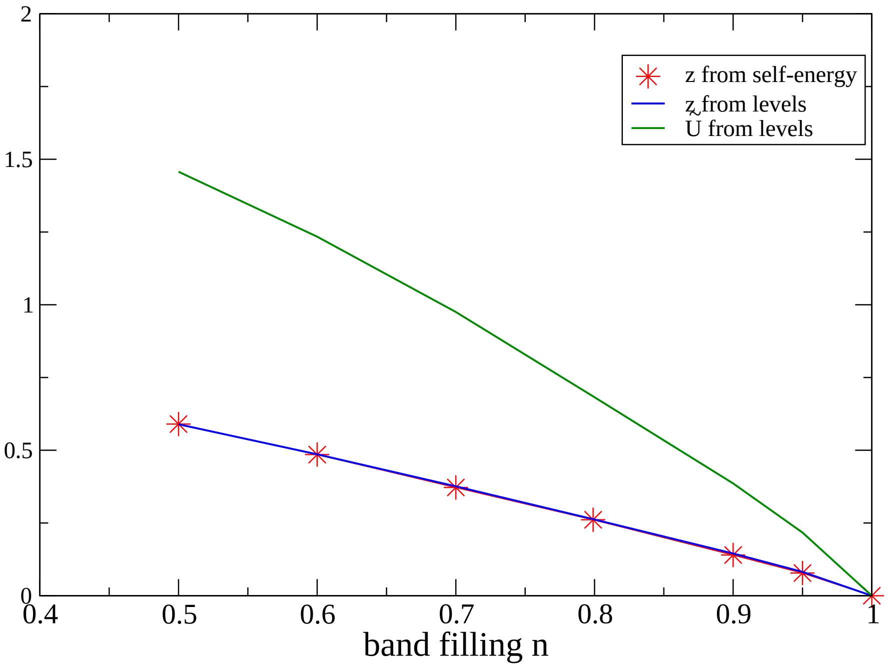

Again complete agreement with z calculated from the self-energy and from the renormalized parameters. $\tilde{U}$ monotonically increase with doping. Again the ratio of $\tilde{U}\tilde{\rho}(0) \to 0.84$ as $n \to 1$, indicating a single energy scale in the strong correlation limit.

As $(1 + \tilde{U}\tilde{\rho}(0)) = 1.84 < 2$, reduced moment?

Spin and Charge Dynamics for Lattice Models

$$\chi_s(\mathbf{q},\omega) = \frac{1}{2}\frac{\tilde{\Pi}^{p\uparrow}_{h\downarrow}(\mathbf{q},\omega)}{1-\tilde{U}^{p\uparrow}_{h\downarrow}\tilde{\Pi}^{p\uparrow}_{h\downarrow}(\mathbf{q},\omega)},$$

$$\chi_c(\mathbf{q},\omega) = \frac{1}{2}\frac{\tilde{\Pi}^{p\uparrow}_{p\downarrow}(\mathbf{q},\omega)}{1-\tilde{U}^{p\uparrow}_{p\downarrow}\tilde{\Pi}^{p\uparrow}_{p\downarrow}(\mathbf{q},\omega)}$$

where $U^{p\uparrow}_{h\downarrow}$ and $U^{p\uparrow}_{p\downarrow}$ the irreducible vertices, which in DMFT are local quantities.

Contribution to Self-energy from Scattering with Spin Fluctuations

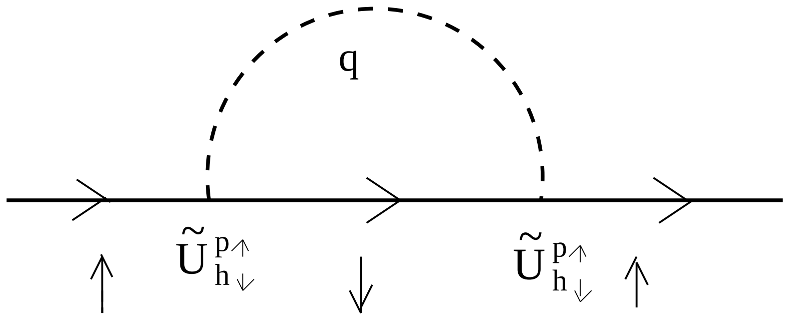

Contribution to self-energy $\Sigma(\omega,\mathbf{k})$ from scattering with a transverse spin fluctuations. Note the self-energy now has a $\mathbf{k}$-dependence because it goes beyond DMFT.

Can we use temperature dependent running coupling constants?

The relation used in NRG calculations:

$$T_N = \eta D \Lambda^{-(N-1)/2}$$

Allows one to deduce $\tilde{\epsilon}_d(T)$, $\tilde{\Delta}(T)$ and $\tilde{U}(T)$ from $\tilde{\Delta}(N)$ and $\tilde{\epsilon}_d(N)$ and $\tilde{U}(N)$.

$$\chi_s(T) = \frac{(g\mu_{\rm B})^2}{2}\tilde{\rho}_d(0,T)(1+\tilde{U}(T)\tilde{\rho}_d(0,T))$$

with $\tilde{\rho}_d(0,T)$ given by

$$\tilde{\rho}_d(0,T) = -\int_{-\infty}^{\infty}\tilde{\rho}(\omega,T)\frac{\partial f(\omega)}{\partial\omega}d\omega$$

where $f(\omega) = 1/(e^{\omega/T}+1)$, and $\tilde{\rho}(\omega,T)$ is the free quasiparticle density of states with parameters $\tilde{\Delta}(T)$ and $\tilde{\epsilon}_d(T)$ and $\tilde{U}(T)$.

In mean field or Hartree-Fock theory we have

$$\tilde{U}_{\rm mf}(T) = U/(1-U\tilde{\rho}_{d,{\rm mf}}(0,T))$$

and substituting this in the expression above gives the mean field result,

$$\chi_s(T)/(g\mu_{\rm B})^2 = 0.5\tilde{\rho}_{d,{\rm mf}}(0,T)/(1-U\tilde{\rho}_{d,{\rm mf}}(0,T))$$

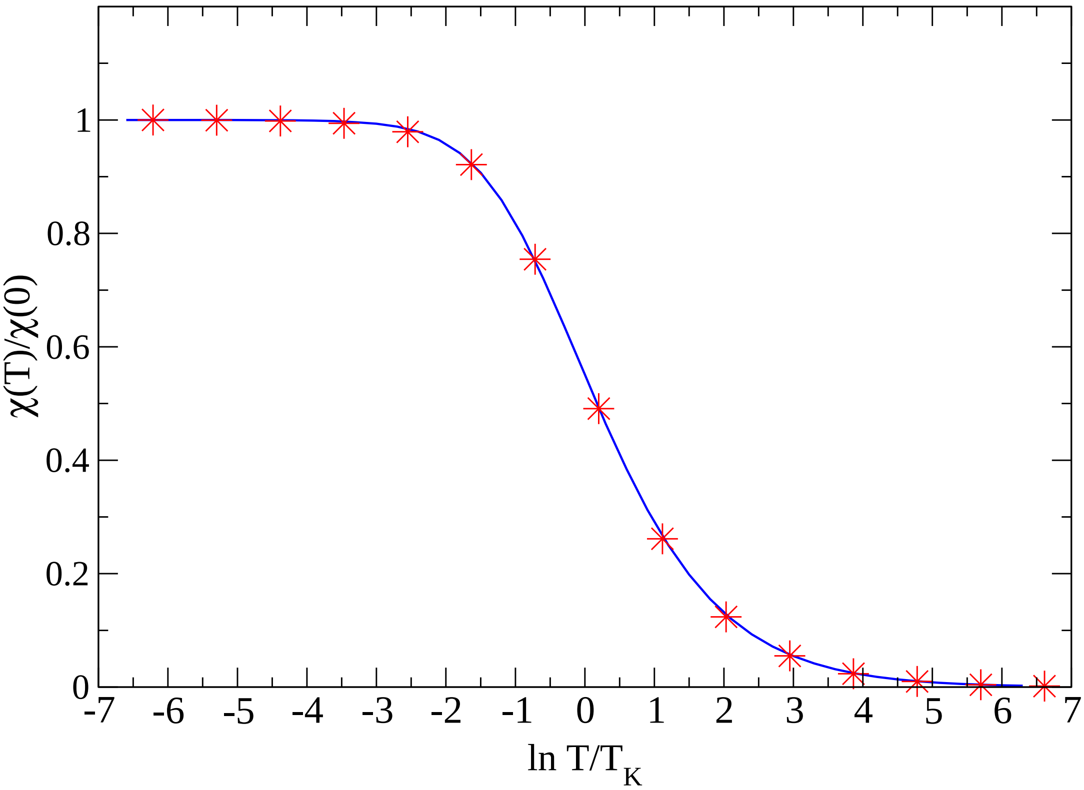

Susceptibility as a function of T

The full curve corresponds to Bethe ansatz results for the s-d model and the stars to results using temperature dependent renormalized parameters for the Anderson model for $U/\pi\Delta = 5$.

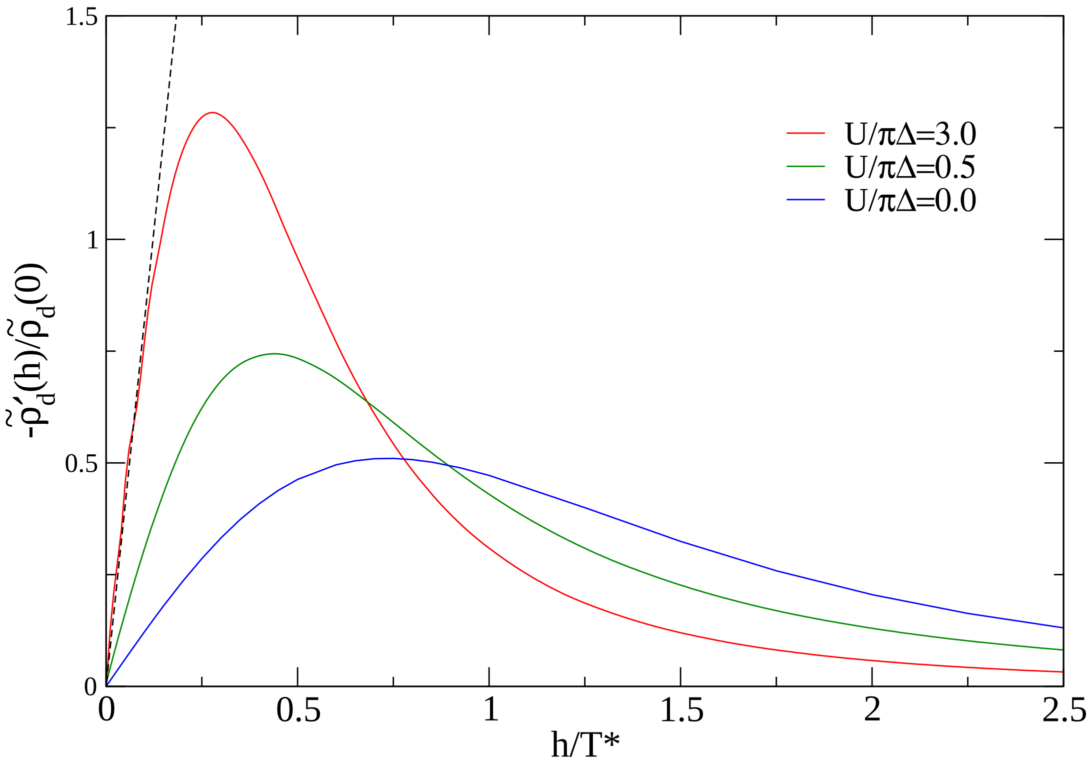

Susceptibility:

$$\chi_s(0,h) - \chi_s(T,h) = -\frac{\pi^2}{12}T^2\frac{\partial^2 \tilde{\rho}_{\rm d}(0,h)}{\partial h^2} = c_\chi(h)\left(\frac{T}{T^*}\right)^2$$

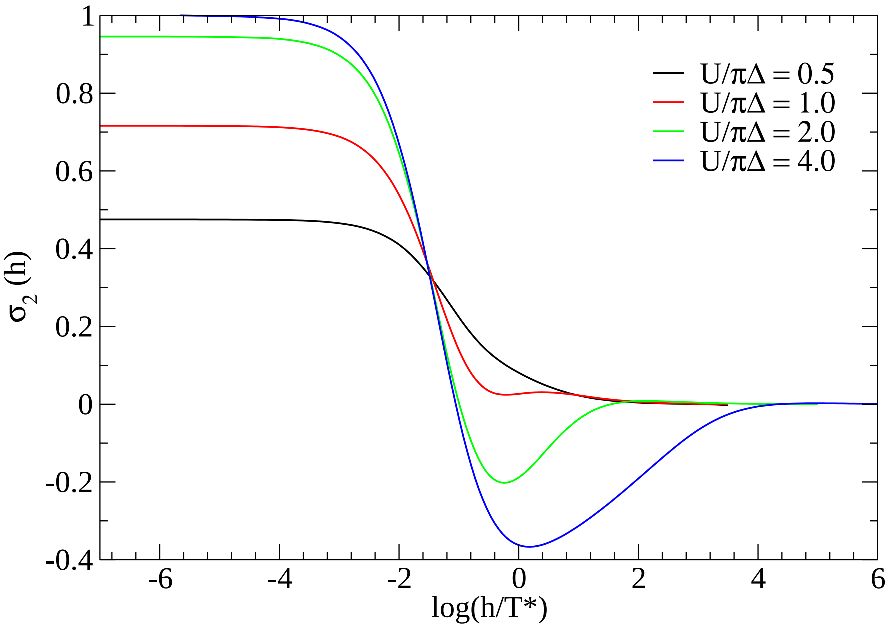

Impurity contribution to conductivity:

$$\sigma(h,T) = \sigma(h,0)\left\{1 + \sigma_2(h)\left(\frac{\pi T}{\tilde{\Delta}(h)}\right)^2 + \mathrm{O}(T^4)\right\}$$

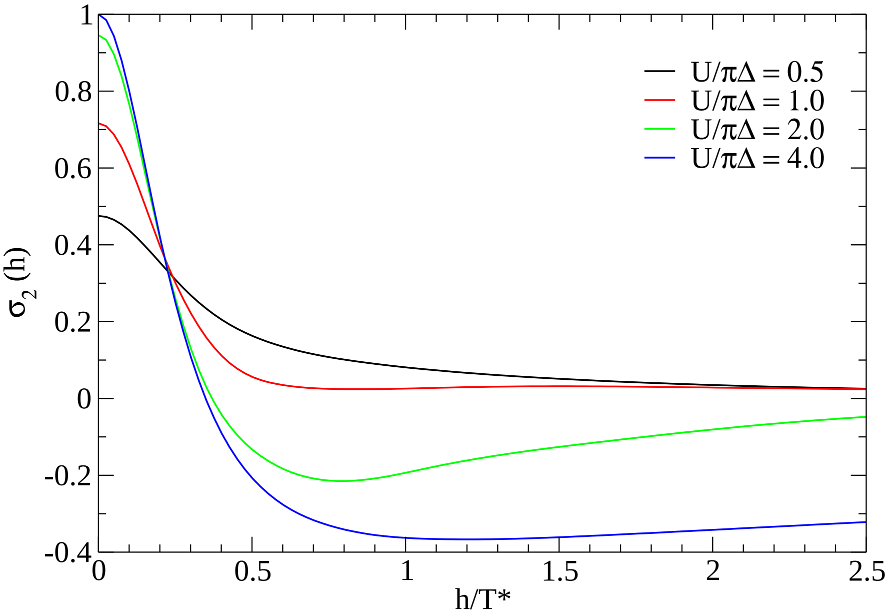

Impurity contribution to conductivity for range $0 < h < 2.5T^*$.

$\sigma_2(h)$ changes sign at $h = h_c$ in the local moment regime.

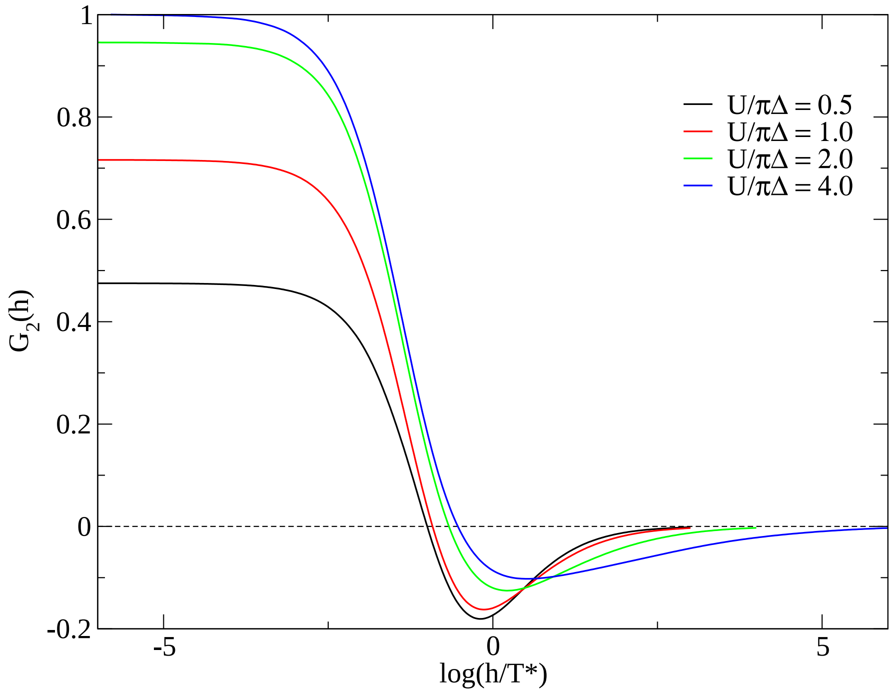

Conductance of quantum dot:

$$G(T,h) = G(0,h)\left(1 - G_2(h)\left(\frac{\pi T}{\tilde{\Delta}(h)}\right)^2\right)$$

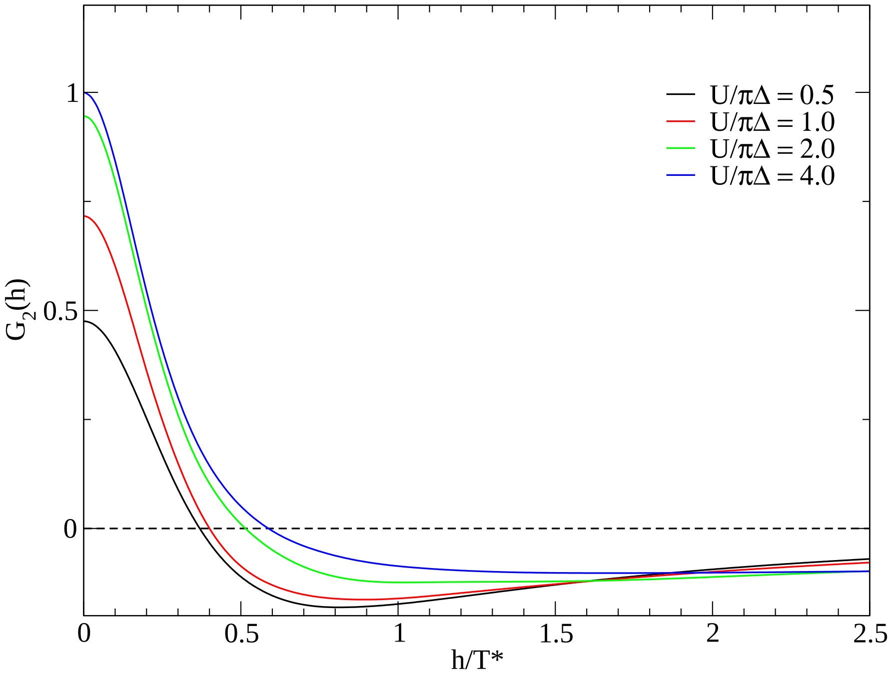

Conductance of quantum dot in range $0 < h < 2.5T^*$

In this case $G_2(h)$ changes sign in all cases.

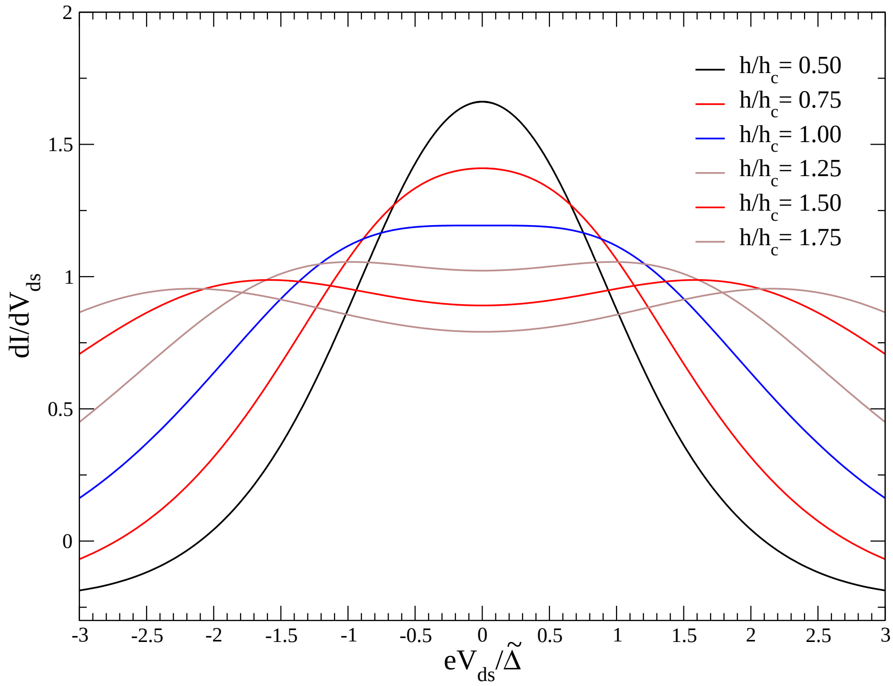

Conductance of quantum dot at $T = 0$

$$\frac{dI}{dV_{ds}} = G_0(h)\left(1 + A_2(h)V_{ds}^2 + \mathrm{O}(V_{ds}^4)\right)$$

There is a critical field h_c for two peaks to be seen in the differential conductance of a quantum dot at a function of the bias voltage V_{ds}. This occurs when $A_2(h)$ changes sign.

Differential Conductance through a Quantum Dot

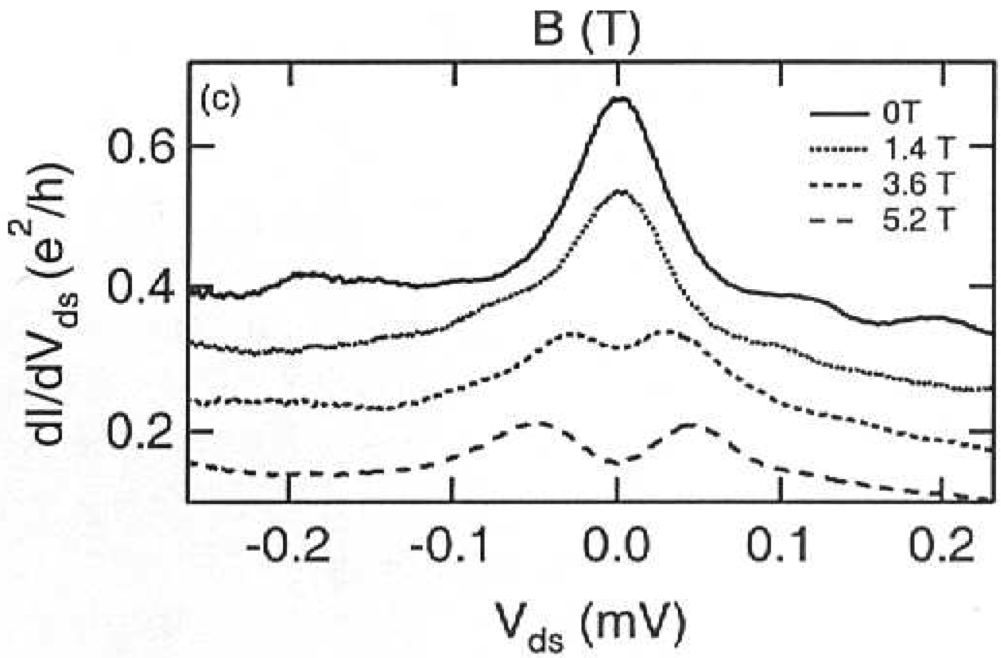

In the Kondo regime the differential conductance as a function of the bias voltage V_{ds} shows the evolution of a two-peak structure with increasing magnetic field H.

Taken from the paper of S.Amasha, I.J. Gelfand, M.A. Kastner and A. Kogan, cond-mat/0411485.